Revisiting the notion of deleterious sweeps

Parul Johri[1,‡], Brian Charlesworth[2,‡], Emma K. Howell[1], Michael Lynch[1,3,*], and Jeffrey D. Jensen[1,*]

[1]School of Life Sciences, Arizona State University, Tempe, AZ 85287, United States
[2]Institute of Evolutionary Biology, School of Biological Sciences, University of Edinburgh, EH9 3FL, United Kingdom
[3]Center for Mechanisms of Evolution, The Biodesign Institute, Arizona State University, Tempe, AZ, United States

[‡] authors contributed equally
[*]co-corresponding authors

keywords: population genetics, selective sweeps, genetic hitchhiking

ABSTRACT

It has previously been shown that, conditional on its fixation, the time to fixation of a semi-dominant deleterious autosomal mutation in a randomly mating population is the same as that of an advantageous mutation. This result implies that deleterious mutations may generate selective sweep effects. Although their fixation probabilities greatly differ, the much larger input of deleterious relative to beneficial mutations suggests that this phenomenon could be important. We here examine how the fixation of mildly deleterious mutations affects levels and patterns of polymorphism at linked sites, and how this class of sites may contribute to divergence between-populations and species. We find that, while deleterious sweeps are unlikely to represent a significant proportion of outliers in polymorphism-based genomic scans within populations, minor shifts in the frequencies of deleterious mutations can influence the proportions of private variants and the value of F_{ST} after a recent population split. As sites subject to deleterious mutations are necessarily found in functional genomic regions, interpretations in terms of recurrent positive selection may require reconsideration.

INTRODUCTION

Among the most important results in theoretical population genetics, now nearly a century old, are the fixation probabilities of new beneficial and deleterious mutations, which were obtained by Fisher (1922, 1930), Haldane (1927), and Wright (1931), using different approaches. Their results were later generalized by Kimura (1957, 1962, 1964), using the backward diffusion equation. A somewhat lesser known result concerns the trajectories of these selected mutations. Specifically, Maruyama & Kimura (1974) found that, conditional on fixation, the time that a beneficial autosomal mutation with selection coefficient $+s$ and dominance coefficient h spends in a given interval of allele frequency in a randomly mating population is the same as that for a deleterious mutation with selection coefficient $-s$ and dominance coefficient $1 - h$, provided that the conditions for the validity of the diffusion equation approximation hold. Thus, given that the effects of selective sweeps on variability at linked neutral sites are related to their speed of transit through a population (Maynard Smith & Haigh 1974; Stephan 2019), the fixation of a deleterious mutation by genetic drift can generate a similar selective sweep effect to that caused by the fixation of a beneficial mutation, for mutations with the same magnitude of selection coefficient. Moreover, Tajima (1990) demonstrated that, on average, there is a ~42% mean reduction in diversity at a site where a neutral mutation has recently become fixed by genetic drift. While the mean time to fixation for this class of mutation is well known to be $4N_e$ generations (Kimura & Ohta 1969); this is of course associated with a wide variance of approximately $4.64N_e^2$ (Kimura 1970), such that neutral mutations may also fix relatively rapidly (in less than N_e generations) and generate an appreciable but highly localized sweep effect (see Tables 1 and 2 of Tajima 1990).

Naturally, the probabilities of deleterious and beneficial fixations differ strongly. However, given that the input of deleterious mutations is much higher than the input of beneficial mutations

each generation (see reviews by Eyre-Walker & Keightley 2007; Bank *et al.* 2014a), the potential contribution of such deleterious sweeps to levels and patterns of nucleotide variation, as well as divergence between populations and species, remains an important open question (Charlesworth 2020a). An alternative way of viewing this issue, as discussed by Gillespie (1994) and Charlesworth & Eyre-Walker (2007), is that under a model of constant selection and reversible mutation between two alternative nucleotide variants, statistical equilibrium with respect to the frequencies of sites fixed for the alternatives implies equal rates of beneficial and deleterious substitutions per unit time. It is important to note, however, that only deleterious mutations with selection coefficients on the order of the reciprocal of the population size have significant probabilities of fixation (Fisher 1930; Kimura 1964), implying that the substitutions concerned involve only very weakly selected mutations. The effects on diversity statistics of sweeps of very weakly selected mutations, including those of deleterious mutations, appears to have been investigated previously only by Mafessoni & Lachmann (2015).

A starting point for investigating this problem is the distribution of fitness effects of new mutations (the DFE). There is substantial evidence from both empirical and experimental studies that the DFE of new mutations is bimodal - consisting of a strongly deleterious mode, and a weakly deleterious / neutral mode that may contain a beneficial tail under certain conditions (*e.g.,* Crow 1993; Lynch *et al.* 1999; Sanjuán 2010; Jacquier *et al.* 2013; Bank *et al.* 2014b). While the calculations and simulations presented below represent a general approach to addressing this topic, we have necessarily chosen a specific DFE realization and species for illustration. Specifically, Johri *et al.* (2020) recently presented an approximate Bayesian (ABC) approach, which represents the first joint-estimator of the DFE shape together with population history that corrects for the effects of background selection (BGS; Charlesworth *et al.* 1993). They estimated that a substantial

98 proportion of new mutations in coding regions have mildly deleterious effects on fitness,
99 emphasizing the importance of further understanding the consequences of such mutations in
100 dictating observed polymorphism and divergence. Furthermore, they found it unnecessary to
101 invoke a beneficial mutational class in order to fit the data from the African population of
102 *Drosophila melanogaster* that they considered.

103 This analysis provides a basis for exploring the possible implications of sweeps of
104 deleterious mutations, a topic that has been rather neglected. Here, we re-examine this question,
105 considering both single and recurrent substitution models, which we use to examine the possibility
106 that genomic scans for positive selection may in fact also be identifying deleterious fixations, when
107 based on: a) levels and patterns of variation; b) population differentiation; and c) species-level
108 divergence. Our results suggest that, while this phenomenon is unlikely to be a major factor in
109 polymorphism-based scans, it may be a serious confounder in among-population-based analyses.

110

111 **METHODS**

112 Analytical calculations

113 For convenience, we assume a Wright-Fisher population of N randomly mating individuals
114 throughout the analytical section. The selection coefficient for homozygotes is denoted by s, with
115 $s = s_a$ or $s = -s_d$ (s_a and $s_d > 0$), representing selection for and against homozygotes, respectively.
116 In particular, the distribution of fitness effects (DFE) for semi-dominant deleterious mutations is
117 assumed to be discrete, with four fixed classes of mutations given by $0 < 2Ns_d \leq 1$, $1 < Ns_d \leq 10$,
118 $10 < 2Ns_d \leq 100$ and $100 < 2Ns_d \leq 2N$, where mutations are assumed to follow a uniform
119 distribution within each class. These assumptions concerning the distribution of s_d were made in
120 order to simplify integration over the DFE (Johri *et al*. 2020).

121 *Probability of fixation*: The fixation probability (P_{fix}) of a new semi-dominant mutation with an
122 initial frequency of $1/2N$ in a Wright-Fisher population of size N was calculated using Equation
123 10 of Kimura (1962):

124 $$P_{fix} = \frac{1 - e^{s}}{1 - e^{2Ns}} \approx \frac{s}{e^{2Ns} - 1} \qquad (1)$$

125 Note that this equation assumes demographic equilibrium and independence between the selected
126 sites, as well as $|s| << 1$.

127 *Contributions to divergence*: Under the DFE model described above, the number of fixations N_{fix}
128 (i) expected per generation per site for a given DFE class i of deleterious mutations is given by
129 the following expression:

130 $$N_{fix}(i) = 2N\mu \times f_i \times \frac{1}{s_{d2} - s_{d1}} \int_{s_{d1}}^{s_{d2}} P_{fix}(s)ds \qquad (2)$$

131 where μ is the total mutation rate per site per generation, f_i represents the proportion of new
132 mutations belonging to the ith DFE class and s_{d2} and s_{d1} represent the upper and lower bounds to
133 the DFE class, respectively. The integral in equation (2) was evaluated analytically by means of
134 an infinite series representation (derivation provided in Appendix 1), which was validated using
135 the "integrate" function in R (R Core Team 2018).

136 *Waiting and fixation times*: The waiting time (t_w) between fixations under a Poisson process was
137 calculated as follows:

138 $$t_w = \frac{1}{L \times N_{fix}} \qquad (3)$$

139 where L represents the number of functional sites under consideration.

The expected time to fixation of a semi-dominant mutation was calculated by numerically integrating equation (17) of Kimura & Ohta (1969), using Simpson's rule (Atkinson 1989).

Reduction in diversity due to a single sweep: The expected reduction in pairwise nucleotide site diversity at the end of a sweep ($-\Delta\pi$), relative to the diversity in the absence of selection, was calculated using equation (14a) of Charlesworth (2020b) for a non-zero rate of recombination (omitting a factor that describes the effect of background selection):

$$-\Delta\pi = (1 - P_r) - T_s - P_{rs}T_d - (P_r - P_{rs})T_r \qquad (4)$$

where T_s is the mean coalescent time (in units of N) for a pair of alleles sampled at the end of a sweep, T_d is the duration of the deterministic phase of the sweep (*i.e.*, excluding the initial and final stochastic phases) in units of N, T_r is the mean time to a recombination event during the sweep, conditioned on the occurrence of a recombination event; P_r is the probability of at least one recombination event transferring a sampled allele onto the wild-type background during the sweep, and P_{rs} is the probability that there is only a single such recombination event. For large values of the ratio of the rate of recombination between the neutral and selected site (r) to the magnitude of the selection coefficient, this expression can become negative, in which case it is reset to zero.

We also used simulations based on equations (27) of Tajima (1990), which provide recursion equations for the expectation of the pairwise diversity at a neutral locus linked to a selected locus, conditional on a given trajectory of allele frequency change at the selected locus, as described by Charlesworth (2020b). These equations require only the validity of the diffusion equation approximation. Binomial sampling of allele frequencies post-selection in each generation was used to generate the trajectories of change at the selected locus, using the standard selection equation for a single locus to calculate the deterministic change in allele frequency each

162 generation. Application of the recursion equations to a trajectory of allele-frequency change
163 simulated in this way gives one realization of $\Delta\pi$; and the overall expected value of $\Delta\pi$ can be
164 obtained from the mean of the simulated values over a large number of replicates. It was found
165 that 1000 replicates gave very accurate estimates of $\Delta\pi$, with ratios of the standard errors to the
166 means of < 5% for the parameter sets used here.

167

168 *Population genetic parameters used for analytical calculations*: The parameters for the
169 calculations were chosen to match those estimated from *D. melanogaster* populations, estimated
170 from exonic sites. Mutations occurred at a rate μ per basepair, and were assumed to be a mixture
171 of neutral, nearly neutral and weakly deleterious mutations. For this analysis; $\mu = 3 \times 10^{-9}$ per
172 basepair (bp) per generation (Keightley *et al.* 2009, 2014). The sex-averaged rate of crossing over
173 per bp (r_c) was assumed to be equal to 10^{-8} per generation (Fiston-Lavier *et al*. 2010), the effective
174 population size was 10^6 (Arguello *et al*. 2019; Johri *et al*. 2020), and 10 generations per year were
175 assumed. Given estimates of neutral divergence between *D. melanogaster* and *D. simulans*, this
176 means that $t \sim 21.3 \times 10^6$ generations elapsed since their common ancestor (Li *et al*. 1999; Halligan
177 & Keightley 2006), corresponding to 2.13 M years.

178 Because non-crossover associated gene conversion is an important source of recombination
179 between closely linked sites in *Drosophila*, it was assumed to occur uniformly across the genome,
180 independently of local differences in the rate of crossing over, as indicated by the data on *D,*
181 *melanogaster* (Comeron *et al*. 2012; Miller *et al*. 2016). The sex-averaged rate of initiation per bp
182 of conversion events was $r_g = 10^{-8}$ per bp per generation, and there was an exponential distribution
183 of tract length with a mean of $d_g = 440$ bp (Comeron *et al*. 2012; Miller *et al*. 2016). The net rate

184 of recombination between sites separated by z bp, $r(z)$, is the sum of the contributions from
185 crossing over and non-crossover gene conversion, given by the formula of Frisse *et al*. (2001):

186 $$r(z) = r_c z + 2r_g d_g[1 - \exp\left(-\frac{z}{d_g}\right)] \qquad (5)$$

187 For some of the results presented below, only the net rate of recombination r, or its value
188 scaled by the effective population size, $\rho = 2Nr$, was used. In the presence of gene conversion
189 with the parameters described above, the corresponding value of z can then be obtained by
190 Newton-Raphson iteration of the equation $r(z) - r = 0$, assuming that the rate of gene conversion
191 does not vary with the rate of crossing over,

192 Simulations

193 *Simulating individual fixations in a single population*: SLiM 3.3.1 (Haller & Messer 2019) was
194 used to simulate a genomic element of length 10 kb. For the single sweep model, in order to
195 quantify the hitchhiking effect of a single fixation, selection only acted on a single site in the
196 middle of the region, with all other sites evolving neutrally. Simulations were performed for five
197 different values of the scaled selection coefficient: $2Ns = 0, -1, +1, -5$, and $+5$. Population genetic
198 parameters resembling those of *D. melanogaster* were utilized (as defined above) for illustrative
199 purposes. In order to perform simulations efficiently, population size was scaled down by a factor
200 of 100 while the mutation and recombination rates were correspondingly scaled up by the same
201 factor. Simulations were run for a burn-in period of 10^5 generations ($10N_{\text{sim}}$) after which a
202 mutation with a scaled selection coefficient of $2Ns$ was introduced at the selected site. Simulations
203 in which the introduced mutation reached fixation were retained for analysis. Fifty diploid

204 individuals were sampled at the completion of the simulations, and population genetic summary
205 statistics were calculated using *Pylibseq* (Thornton 2003).

206 *Simulating multiple populations and F_{ST}-based analyses*: Based on a recently inferred
207 demographic history of African and European populations of *D. melanogaster* using populations
208 sampled from Beijing, the Netherlands, and Zimbabwe (Arguello *et al*. 2019), an ancestral
209 population of size of 1.95×10^6 was simulated, which split into two populations (6.62×10^4
210 generations ago) of constant size: 3.91×10^6 and 4.73×10^5, representing African and European
211 populations, respectively. Note that, although Arguello *et al*. inferred recent growth in both
212 populations, we have assumed constant sizes in order to avoid confounding effects of such growth
213 on the fixation probabilities of mutations, and we also assumed no migration between the two
214 populations. For the purpose of F_{ST} analyses, a functional region of size 10 kb was simulated, in
215 which mutations had selection coefficients given by the DFE inferred in Johri *et al.* (2020).
216 Specifically, the DFE was given by a discrete distribution of four fixed bins with 24.7% of
217 mutations belonging to the effectively neutral class (f_0: $0 \leq 2Ns_d < 1$), 49.4% to the weakly
218 deleterious class (f_1: $1 \leq 2Ns_d < 10$), 3.9% to the moderately deleterious class (f_2: $10 \leq 2Ns_d <$
219 100), and 21.9% to the strongly deleterious class of mutations (f_3: $100 < 2Ns_d \leq 2N$).

220 In this two-population framework, four separate scenarios were tested: 1) the DFE
221 remained scaled to the ancestral population size (making selection effectively weaker in the
222 smaller derived (European) population); 2) the DFE was rescaled after the population split with
223 respect to subpopulation-specific sizes (*i.e*., both populations experienced equal proportions of
224 mutations belonging to each DFE class as defined in terms of $2Ns_d$), such that selection was
225 equally strong in both populations - this is an arbitrary biological model that is simply chosen for
226 comparison, as one would naturally expect selection to be effectively weaker in the derived

227 population as in scenario 1; 3) in addition to this neutral and deleterious DFE, 1% of all mutations
228 were mildly beneficial with selective effects drawn uniformly from the interval $1 \leq 2Ns_a \leq 10$,
229 where s_a is the increase in fitness of the mutant homozygote; and 4) in addition to this neutral and
230 deleterious DFE, 1% of all mutations were strongly beneficial with $2Ns_a = 1000$. In scenarios 3
231 and 4, the deleterious and beneficial DFEs were scaled to the respective sizes of each population
232 post-split, so that the proportions of beneficial mutations were the same in the two populations. In
233 order to assess the role of population bottlenecks in generating neutral outliers, a fifth scenario was
234 simulated in which there was no selection and the demographic history was that inferred by Li &
235 Stephan (2006) - a model that involves a much larger size reduction than inferred in the Arguello
236 *et al*. (2019) model utilized above. The parameters of both demographic models are provided in
237 Supp Table 1.

238 Fifty diploid individuals were sampled from both populations in order to calculate F_{ST}. All
239 sites that would be considered polymorphic in the metapopulation were used to calculate F_{ST} (*i.e.*,
240 sites fixed either in one population or both populations (for different alleles) were also included in
241 F_{ST} calculations). F_{ST} was calculated in sliding windows across the genomic region for a) windows
242 containing a constant number of SNPs using the package PopGenome (Pfeifer *et al*. 2014) in R,
243 and b) for windows representing the same total number of bases using *Pylibseq* 0.2.3 (Thornton
244 2003). F_{ST} was calculated for both cases by the method of Hudson *et al*. (1992). F_{ST} was also
245 calculated individually for different mutation types (*i.e.*, for neutral, weakly deleterious and
246 beneficial mutations, by simply restricting the calculations to segregating sites of the specific
247 mutation type). Although there will be an upper bound to the F_{ST} values obtained in this way,
248 which is determined by the frequency of the most frequent allele in the metapopulation (Jakobsson

249 *et al*. 2013), the detection of outliers should not be affected by this procedure and should mimic
250 the scenario for natural populations of *Drosophila*.

251 *Simulating multiple species, and divergence-based analyses:* McDonald-Kreitman (MK) tests
252 (McDonald & Kreitman 1991) were performed to investigate the degree to which substitutions of
253 mildly deleterious mutations might affect the inference of divergence due to positive selection. A
254 population resembling a *D. melanogaster* African population was simulated under demographic
255 equilibrium. Ten independent replicates of a 10-kb protein-coding region were considered such
256 that every third position was neutral (representing synonymous sites) while all other sites
257 represented nonsynonymous positions. Nonsynonymous sites experienced purifying selection
258 given by a DFE that comprised only the non-neutral bins (*i.e.,* f_1, f_2, and f_3, in the same proportions
259 described above), while the neutral sites experienced mutations that belonged to class f_0. For
260 comparison, simulations were performed in which 10% or 20% of nonsynonymous mutations were
261 also neutral. In all cases, the simulation was run for $20N$ generations (where $N = 10^4$). The number
262 of segregating nonsynonymous (P_N) and synonymous (P_S) sites were estimated by sampling 50
263 diploid individuals from the population from the functional and neutral regions respectively. The
264 number of fixed substitutions occurring at the functional sites (D_N) and neutral sites (D_S) were
265 calculated post burn-in (*i.e.*, after $10N$ generations), and then rescaled to the number of generations
266 since the *D. melanogaster* ancestor.

267 In order to correct for mildly deleterious mutations segregating in populations, the
268 proportion of adaptive substitutions (α) was also inferred by implementing a variant of the test
269 referred to as the asymptotic MK test. Messer & Petrov (2013) suggested plotting the derived
270 allele frequency (x) of variants against α inferred using the number of segregating sites ($P(x)$) at

271 that derived allele frequency (*i.e.*, $\alpha(x) = \frac{P(x)_N}{P(x)_S} \times \frac{D_S}{D_N}$), and showed that the asymptote of this

272 curve would tend towards the true value of α. The asymptotic MK test was performed using a

273 web-based tool available at: http://benhaller.com/messerlab/asymptoticMK.html (Haller &

274 Messer 2017). For the purpose of the asymptotic MK test, values of P_N/P_S were binned with a

275 bin size of 0.05, and the curve-fitting (of $\alpha(x)$ with respect to x) was restricted to derived allele

276 frequencies between 0.1-1.0

277

278 **RESULTS & DISCUSSION**

279 Theoretical expectations

280 As has been long appreciated (Fisher 1930; Wright 1931), equation (1) implies that the probability

281 of fixation of a mutation in the strongly deleterious DFE classes is vanishingly small. However,

282 the weakly deleterious class may contribute substantially to divergence (Figure 1a). We derived

283 an analytical approximation for the probability of fixation for mutations with a DFE represented

284 as a combination of four non-overlapping uniform distributions (see Methods and Appendix 1). In

285 a Wright-Fisher population, the ratio of the mean probability of fixation of mutations with fitness

286 effects between $1 < 2Ns_d \leq 5$, relative to the probability of fixation of effectively neutral mutations

287 ($0 < 2Ns_d \leq 1$), is 0.27 (note that the value of N is irrelevant if the diffusion approximation holds).

288 This ratio rapidly declines to 0.01 for mutations with fitness effects $5 < 2Ns_d \leq 10$ (Figure 1a).

289 Taking the recently estimated DFE for the Zambian *D. melanogaster* population (Johri *et*

290 *al*., 2020) as an example, a question of interest concerns the probabilities of fixation of different

291 classes of mutations and their contributions to population- and species-level divergence (Supp

292 Figure 1). In the absence of positive selection, the weakly deleterious class of mutations would be

293 expected to contribute 7.2% of the total divergence in exonic regions, while effectively neutral
294 mutations would be expected to contribute 92.8%. If we were to assume that approximately 50%
295 of all substitutions in *Drosophila* have been caused by positive selection (Eyre-Walker and
296 Keightley 2009; Campos *et al*. 2017), weakly deleterious mutations are still likely to have
297 contributed 3.5% of the total divergence in functional regions and possibly much more in regions
298 experiencing reduced selective constraints.
299
300 Hitchhiking effects of deleterious sweeps: levels and patterns of variation
301 We next considered the fixation times of these mutations contributing to divergence, as well as the
302 expected waiting time between fixations. Using population parameters relevant for *D.*
303 *melanogaster* (see Methods), the neutral and deleterious DFE of Johri *et al.* (2020), and assuming
304 that 60% of the *D. melanogaster* genome (of size 140 Mb) is functional, equation (3) shows that
305 the genome-wide waiting time between successive weakly deleterious fixations is ~ 83
306 generations. Hence, the ~2.13 million years estimated for the time since the *D. melanogaster* and
307 *D. simulans* split is expected to equate to many such fixations.
308 As expected, there is no significant difference (p = 0.16; Student's t-test) in fixation times
309 between the mildly beneficial (3.2N generations; SD: 1.5N) *vs* mildly deleterious mutations (2.9N
310 generations; SD: 1.1N) with the same fitness effects ($2Ns_a = 2Ns_d = 5$) (Supp Table 2). Importantly
311 however, the variance in fixation times of weakly selected mutations is extremely large, such that
312 the faster tails of the fixation time distributions for both $2Ns_d$ = 5 and $2Ns$ = 0 occupy ~N
313 generations, which corresponds to a sweep effect of the same size as the mean for $2Ns_a$ = 30
314 (Figure 1b). In other words, weakly deleterious and neutral fixations can match the sweep effects
315 of comparatively strongly selected beneficial fixations.

316 We evaluated the impact of these fixations on observed genomic variation in two ways.
317 The first corresponds to a model of a single sweep event, which is relevant to the literature on
318 detecting signatures of individual fixations, as done in genomic scans for positively selected loci
319 (*e.g.*, Harr *et al.* 2002; Glinka *et al.* 2003; Haddrill *et al.* 2005; Nielsen *et al.* 2005; see also Jensen
320 2009; Stephan 2019). Such scans operate under the assumption that the selective sweeps in
321 question have achieved fixation immediately prior to sampling, due to the rapid loss of signal as
322 the time since fixation increases (Kim & Stephan 2002; Przeworski 2002). The second corresponds
323 to a recurrent substitution model, which is relevant to the recurrent sweep literature that attempts
324 to quantify the effect of selective sweeps on genome-wide patterns of variability and their relation
325 to rates of recombination (*e.g.*, Wiehe & Stephan 1993; Kim 2006; Andolfatto 2007; Macpherson
326 *et al.* 2007; Jensen *et al.* 2008; Campos & Charlesworth 2019; Charlesworth 2020b; see review by
327 Sella *et al.* 2009).

328 The reduction of diversity resulting from the fixation of a mildly deleterious or beneficial
329 semi-dominant mutation with a very small selective effect is not expected to be substantially
330 different from that caused by the fixation of a selectively neutral mutation (Tajima 1990). The
331 widely-used approximation of Barton (2000) for the reduction in diversity relative to neutrality
332 caused by the sweep of a semi-dominant mutation, $\Delta\pi = (2Ns_a)^{(-4r/s)}$, suggests that, when $2Ns_a$
333 $= 5$, diversity will only be reduced by more than 20% in a region for which $r/s \leq 0.2$,
334 corresponding to approximately 20 bp for a typical *D. melanogaster* recombination rate of $3 \times 10^{-}$
335 ^{8} per bp, including the contribution from gene conversion as given by equation (6), and assuming
336 an effective population size of $\geq 10^6$.

337 However, this formula assumes that fixations are so fast that swept alleles that have failed
338 to recombine onto a wild-type background experience no coalescent events during the duration of

339 the sweep (Hartfield & Bataillon 2020; Charlesworth 2020b), which is unlikely to be true for
340 weakly selected mutations. We therefore used equation (4) for analytical predictions (Figure 2,
341 Table 1, Supp Table 3), which is based on the results of Charlesworth (2020b). But this equation
342 is also likely to be inaccurate with weak selection, because it assumes that the trajectory of allele-
343 frequency change is close to that for the deterministic case, except for the initial and final stochastic
344 phases at the two extremes of allele frequencies. We therefore also used simulations based on
345 equations (27) of Tajima (1990) to predict sweep effects, as described in the Methods.

346 With the full simulations of a 10-kb region, in which we assumed a population size of 10^6
347 and mutation rate of 3×10^{-9} /site/generation, with $2Ns_a = 5$ the nucleotide diversity 10 bp ($\sim\rho =$
348 0.2) around the selected site (*i.e.*, 5 bp in both directions) was 0.0058 (SE: 0.0012), corresponding
349 to a reduction of 48% below the neutral value. For $2Ns = 10$, the 10-bp nucleotide diversity was
350 0.0083 (SE: 0.0017), corresponding to a reduction of 69%. The observed reduction in both cases
351 almost fully recovers to the expected level under neutrality within 500 bp ($\rho \approx 10$; Figure 2). A
352 similar pattern is seen in Table 1 and Supp Table 3, which shows both the analytical predictions
353 and those based on Tajima's equations, which agree surprisingly well except at the two highest
354 rates of recombination displayed. For comparison, the results of simulating neutral fixations are
355 also shown in Table 1 and Figure 2. The case with $Ns = 10$ is at the higher limit of what is likely
356 to be produced by sweeps of deleterious mutations, given that the ratio of the fixation probability
357 given by equation (1) to the neutral value of $1/(2N)$ is then approximately 0.0045, compared to
358 0.034 with $Ns = 5$.

359 Mafessoni & Lachmann (2015) showed that that fixations of weakly selected, highly
360 dominant favorable mutations - or highly recessive deleterious mutations - could reduce diversity
361 at linked sites by a *smaller* amount than fixations of neutral mutations, with a maximum effect

362 when $2Ns$ is approximately 2 (and $h = 1$ for favorable mutations, and 0 for deleterious ones). We
363 have confirmed this unexpected observation using Tajima algorithm simulations (Supp Table 4),
364 finding that it exists even for $2Ns = 5$ (Supp Figure 2; Supp Table 4). However, our use of $h =$
365 0.5 and $2Ns \geq 2.5$ means that this phenomenon is absent from the results presented here.

366 Because gene conversion is an important contributor to recombination between closely
367 linked sites (Miller *et al.* 2016), the effects of fixations in the presence of gene conversion are
368 restricted to a region that is about one-third of the distance in the absence of gene conversion
369 (Table 1). Thus, a greater than 20% reduction in nucleotide diversity for $2Ns = 5$ [$2Ns = 10$] was
370 observed up to $\rho = 0.8$ [$\rho = 1.6$], corresponding to 14 bp [27 bp] with gene conversion, and 40 bp
371 [80 bp] without gene conversion. This quite localized effect is similar for weakly beneficial,
372 weakly deleterious, and neutral mutations.

373 Given the relatively faster mean speed (3.1*N* generations) of fixation of weakly selected
374 semi-dominant mutations compared to the neutral expectation (4*N* generations), they should also
375 result in small distortions of the SFS at closely linked neutral sites. We observed a slight skew
376 towards rare variants (as measured by Tajima's *D*, Supp Table 5) restricted to ~50 base pairs from
377 the selected site immediately after fixation (for $2Ns_d = 2Ns_a = 5$). This highly localized
378 distortion of the SFS is probably too weak to play any important role in generating false positives
379 in genomic scans. Indeed, owing to the inherent stochasticity involved in the underlying processes,
380 such scans generally only have power to detect very strongly selected fixations (often requiring
381 values of $2Ns_a > 1000$ in order to observe appreciable true positive rates: Crisci *et al.* 2013).
382 Viewed in another way, given that the false-positive rates associated with genomic scans may often
383 be inflated well-above true-positive rates owing to the underlying demographic history of the
384 population (*e.g.,* Teshima *et al.* 2006; Thornton & Jensen 2007; Crisci *et al.* 2013; Harris *et al.*

385 2018), demography is probably a much stronger confounder than deleterious sweeps in
386 polymorphism-based scans.

387 Finally, using a recurrent fixation model, we considered the steady-state impact of weakly
388 deleterious sweeps (Figure 3). Here we used a model of a gene with five exons of 100 codons each,
389 with 70% of exonic mutations subject to selection, which were separated from each other by 100
390 bp introns, as described by Campos & Charlesworth (2019) and Charlesworth (2020b). Five
391 equally large classes of sites subject to deleterious mutations were modeled, with the lowest scaled
392 selection coefficient being Ns_d = 2.5 and the largest Ns_d = 10; as described above, a uniform
393 distribution of Ns_d values was assumed within each class. The theoretical predictions used the
394 method for predicting the effects of recurrent sweeps of Charlesworth (2020b), based on equation
395 (4) above. For consistency with the simulations of population divergence described below, the
396 population size was assumed to be 1.95×10^6, giving a neutral diversity of 0.0234 with the
397 assumed mutation rate of 3×10^{-9}. Substitution rates of deleterious nonsynonymous mutations
398 were calculated from equations (1) and (2). The expected number of nonsynonymous substitutions
399 per gene over $2N$ generations was 0.506, and the ratio of nonsynonymous to synonymous
400 substitutions was 0.0412, which is somewhat less than half the mean value for comparisons of *D.*
401 *melanogaster* and its close relatives (*e.g.*, Campos *et al.* 2017). The major source of these
402 substitutions is the class with Ns_d between 2.5 and 4.375, which accounts for 76% of all
403 substitutions, reflecting the fact that mutations in this class have the highest fixation probabilities.

404 The results for single sweeps shown in Table 1 suggested that the theoretical predictions
405 will tend to overestimate sweep effects, so that the results in Figure 3 must be treated with some
406 caution. With the standard *D. melanogaster* rate of crossing over per bp of 1×10^{-8}, the mean
407 reduction in nucleotide diversity at synonymous sites caused by deleterious sweeps is

408 approximately 5% with gene conversion and 8% in its absence (Figure 3). For the lowest rates of
409 crossing over and no gene conversion, average reductions can reach ~19%, suggesting that the
410 fixation of mildly deleterious mutations could play a significant role in organisms or genomic
411 regions with highly reduced rates of recombination. In this low recombination environment
412 however, selective interference would also become a factor - which would be expected to
413 accelerate the rate of deleterious fixations, while also making deleterious variants behave more
414 like neutral mutations. Regardless of these details, however, it seems unlikely that substitutions of
415 deleterious mutations will have more than a minor effect on average diversity in the *Drosophila*
416 genome overall, particularly compared with the effects of population history, background
417 selection, and sweeps of positively selected mutations. Furthermore, the findings of Mafessoni &
418 Lachmann (2015) suggest that strongly recessive deleterious mutations will have even smaller
419 effects than those studied here (see Supp. Figure 2).
420
421 <u>The contribution of deleterious mutations to population- and species-level divergence-based scans</u>
422 Given the potentially substantial contribution of the weakly deleterious class to observed fixations,
423 it is also of interest to consider their impact on divergence-based analyses (*e.g.,* methodology
424 related to d_N/d_S) and population differentiation-based scans (*e.g.,* methodology related to F_{ST}). We
425 examined properties related to inferring the proportion of substitutions fixed by positive selection
426 (α) by performing MK tests in the presence of mildly deleterious mutations. Specifically, we
427 simulated two scenarios: 1) 50% of mutations at nonsynonymous sites were weakly deleterious,
428 and 50% were neutral, and 2) nonsynonymous sites experienced deleterious mutations that
429 followed the DFE inferred by Johri *et al*. (2020).

430 Although, as expected, the presence of mildly deleterious mutations substantially increases
431 values of d_N/d_S (Supp Table 6) relative to stronger purifying selection (*i.e.*, larger proportions of
432 moderately and strongly deleterious mutations), it also leads to strongly negative values of α when
433 performing MK tests. This is due to the fact that mildly deleterious mutations often segregate in
434 the population at low frequency, inflating the total number of segregating nonsynonymous
435 polymorphisms (P_N) significantly (Supp Table 6). As such, the presence of mildly deleterious
436 mutations can result in negative values of α in the absence of positive selection, as expected. This
437 is consistent with previous studies that have proposed a derived allele frequency cutoff (Fay *et al*.
438 2001, 2002; Andolfatto 2005; but see Charlesworth & Eyre-Walker 2008) to correct for
439 segregating mildly deleterious alleles, as well as proposed modification of the traditional MK test
440 (*e.g.,* the asymptotic MK test; Messer & Petrov 2013). Nevertheless, under the asymptotic MK
441 test, α remains underestimated (Supp Table 6) when the proportion of mildly deleterious mutations
442 is sufficiently high.

443 In order to study inter-population effects, we simulated a model similar to that recently
444 inferred by Arguello *et al.* (2019), which represents the European and African split of *D.*
445 *melanogaster* (see Methods), and overlaid it with the estimated DFE of Johri *et al.* (2020). Under
446 this model (*i.e.,* in the absence of positive selection), roughly 50% of SNPs identified as F_{ST} outliers
447 (defined as representing the upper 1% or 2.5% tails) are mildly deleterious (Figure 4a; Supp Figure
448 3). Two models of purifying selection are given for comparison (Table 2): 1) a more biologically
449 realistic model in which selection coefficients are scaled to the ancestral population size in defining
450 the DFE classes, such that selection is effectively weaker in the smaller derived population; and 2)
451 an arbitrary model in which the DFE is rescaled such that selective effects are equally strong in
452 the larger ancestral and the smaller derived populations (which, under the chosen demographic

453 model, differ from one another by roughly an order of magnitude). It should be noted that in the
454 model based on Arguello *et al*., the time post-split between the African and European population
455 is extremely brief, such that there are few or no substitutions post-split (Supp Table 7). Thus, F_{ST}
456 values are almost entirely dictated by allele frequency differences with respect to co-segregating
457 mutations (Supp Table 7).

458 Mean F_{ST} values at both neutral and weakly deleterious sites are larger with the rescaled
459 purifying selection model, whereas the unscaled model yields similar values to the purely neutral
460 model (Table 1 and Supp Tables 8, 10). In addition, the frequency of private SNPs at all sites is
461 higher for the rescaled model than the unscaled model, with the neutral model having the lowest
462 value of the three (Supp Table 7). In order to determine whether these weakly deleterious mutations
463 were associated with a decrease in diversity at linked sites, potentially leading to an increase in F_{ST}
464 values (Cruickshank & Hahn 2014), we evaluated the relationship between F_{ST} and nucleotide
465 diversity using neutral variants alone (Supp Figure 4; see also the comparison with directly
466 selected sites in Supp Figures 5-6). The lack of a strong negative correlation suggests that sweep-
467 like effects of deleterious mutations on diversity at linked sites are not primarily responsible for
468 the observed effects on F_{ST} and the frequency of private alleles. In contrast, there is a negative
469 relationship between nucleotide diversity and F_{ST} after the strong population bottleneck
470 represented by the neutral model of Li & Stephan (2006).

471 The lack of sweep-like effects of deleterious mutations is not surprising in view of the time-
472 scale to fixation required for weakly selected mutations, which is of the order of the coalescent
473 time, $2N$ generations; the split times for both the African and European populations are both only
474 a small fraction of their respective coalescent times. Thus, neither new neutral nor weakly
475 deleterious mutations are likely to have reached fixation in either population, consistent with the

476 results shown in the last column of Supp Table 7. In addition, there is no time for large changes in
477 π as a result of the altered N values.

478 Instead, it is more likely that BGS effects on the frequencies of segregating mutations
479 explain these patterns (B = 0.18 and 0.15 in the African and European populations, respectively,
480 obtained from the ratios of neutral π values in the absence of purifying selection to those without:
481 Supp Table 9). In the absence of rescaling of the DFEs for deleterious mutations (the more
482 biologically plausible case), the enhanced N for the African population means that fewer
483 deleterious mutations behave as effectively neutral, so that there is less effect of drift on their
484 frequencies compared with the ancestral population; the reverse is true for the European
485 population. As far as linked neutral variants are concerned, there is likely to be a greater BGS
486 effect in the African than in the ancestral population, and vice-versa for the European population.
487 F_{ST} relative to the purely neutral case is thus subject to two opposing factors, which presumably
488 explains the lack of any strong effect of this model of purifying selection on F_{ST} in Table 2 and
489 Supp Table 8. However, the lower effective population size induced by BGS means that rare
490 variants are more likely to be lost after the population split than under neutrality, explaining the
491 increased proportion of private variants compared with neutrality with purifying selection (Supp
492 Table 7). Because of the effects of BGS, the relative N_e values of the African and European
493 populations are less disparate than the relative N values, so that the African/European ratio of the
494 proportions of private SNPs is smaller than under neutrality (Supp Table 7).

495 The effect of rescaling is to keep the proportion of deleterious mutations that are effectively
496 neutral the same in the two descendant populations, with the absolute strength of selection being
497 higher in the African population, so that overall there is a stronger BGS effect in this population.
498 This results in a higher overall fraction of private SNPs, and a larger enrichment of private SNPs

499 in the African population, compared with the neutral case (Supp Table 7). There is a corresponding
500 increase in mean F_{ST} for both neutral and weakly deleterious variants compared with the neutral
501 case (Table 2 and Supp Table 8).

502 It is also of interest to consider the contribution of deleterious mutations to outliers in the
503 presence of positive selection. When a class of weakly positively selected sites was added to the
504 DFE (*i.e.* beneficial mutations have fitness effects $1 < 2Ns_a \leq 10$, and comprise 1% of new
505 mutations), these adaptive mutations contributed little to the observed outliers (< 5%) - with mildly
506 deleterious and neutral mutations strongly represented amongst outliers (Figure 4b). Conversely,
507 when positive selection is very strong (*i.e.*, mutations have selective effects with $2Ns_a$=1000, and
508 comprise 1% of new mutations), the majority (~75%) of outliers are drawn from this beneficial
509 class (Figure 4c). Yet, even in the presence of this exceptionally strong and frequent positive
510 selection, ~10% of outliers remain in the mildly deleterious class. It is also noteworthy that under
511 this model of strong, recurrent positive selection, little variation within populations is observed,
512 owing to the severity of the selective sweeps (Supp Table 8), and inter-population allele
513 frequencies are only weakly correlated with one another (Supp Table 7).

514 Because any model, including equilibrium neutrality, will have outliers based on empirical
515 *p*-values, we further quantified the properties of outliers (2.5% and 1%) relative to the genome-
516 wide mean. Under models of purifying selection, the values of F_{ST} outliers were ~2.3-4.5 fold
517 larger than mean F_{ST} values (Table 2; Supp Table 10), but differed only slightly from the neutral
518 case. Under the strongly bottlenecked neutral model of Li & Stephan (2006), in which the
519 European population experiences a substantial decrease in population size during the bottleneck,
520 the genome-wide mean F_{ST} values obtained are much higher, as would be expected, though outlier
521 F_{ST} values were smaller in relative magnitude (~1.5-2.7 fold higher than the means). Under models

522 including weak positive selection, only slight increases in genome-wide F_{ST} values were observed;
523 whereas the strong positive selection model greatly increased genome-wide values. However,
524 outlier values under both positive selection models were ~2.4-4.6 fold higher than the respective
525 means. This suggests that recurrent positive selection does not generate substantially larger effect
526 sizes for outlier F_{ST} values than neutrality or purifying selection, although the proportion of outliers
527 is larger with strong positive selection.
528

529 **CONCLUSIONS**

530 In this paper, we have examined the expected impact of deleterious fixations on polymorphism-
531 and divergence-based scans for selection. Amongst the class of weakly deleterious mutations that
532 have some chance of reaching fixation ($1 < 2Ns_d \leq 10$), the resulting sweep effects are highly
533 localized, as expected: on the order of a few dozen base pairs for the parameters considered here.
534 This suggests that deleterious sweeps of this kind are unlikely to be detected in genomic scans
535 based on localized deficits of variation or strongly skewed site frequency spectra. Given the
536 theoretically expected symmetry between beneficial and deleterious sweeps (Maruyama &
537 Kimura 1974; Mafessoni & Lachmann 2015; Charlesworth 2020a), this is expected, as common
538 polymorphism-based methods generally have little power unless selection is exceptionally strong
539 (*e.g.,* Kim & Stephan 2002; Jensen *et al.* 2005; Crisci *et al*. 2013). However, our results suggest
540 that studies which estimate the frequency and strength of classic selective sweeps using patterns
541 of diversity around substitutions (Hernandez *et al*. 2011; Sattath *et al*. 2011; Elyashiv *et al*.
542 2016), which assume that reductions are entirely caused by the fixation of positively selected
543 mutations, ought to take into account reductions caused by neutral and weakly deleterious
544 substitutions.

Furthermore, for among-population comparisons based on F_{ST}, mildly deleterious mutations contribute significantly to observed outliers, even in the presence of positive selection, particularly in the case of a recent population size reduction. This appears to be the true regardless of whether selective effects are equally strong in both populations (Figure 4), or if selection is relaxed in the smaller derived population (Supp Figure 3). Because such effects are localized to functional sites (*i.e.,* those genomic regions experiencing purifying selection), this effect may be particularly pernicious in the sense that this class of outlier will not fall in non-functional regions, where they are often attributed to demographic effects. Rather, owing to the common tendency of constructing biological narratives (true or otherwise) around functional outliers (Pavlidis *et al*. 2012), these results suggest that adaptive story-telling may arise from weakly deleterious outliers. However, we have only considered one specific scenario, and the generality of this conclusion remains to be established.

ACKNOWLEDGMENTS

This work was funded by National Institutes of Health grant R01GM135899 to JDJ.

APPENDIX 1

Calculating the probability of fixation with uniformly distributed fitness effects

For a selection coefficient $s << 1$, the fixation probability of a deleterious mutation when $N_e \neq N$ is approximated by:

$$P_{fix} \approx \frac{s(\frac{N_e}{N})}{\exp(2N_e s)-1} \qquad \text{(A1)}$$

For large N_e, this should be a good approximation, since when $2N_e s \geq 10$, the fixation probability is negligible, so that the contribution from the bin with $2N_e s \geq 10$ can be ignored. For $2N_e s < 10$, s is sufficiently small that this equation is an accurate approximation.

The integral of this expression over a given interval of $2N_e s$ values can be found as follows; for convenience, x is substituted for s and a for $2N_e$. For $a > 0$, we need to evaluate the following indefinite integral:

$$I = \int x(e^{ax} - 1)^{-1} \, \mathrm{d}x$$

Integration by parts give:

$$I = \frac{1}{a}\left[x ln(1 - e^{-ax}) - \int \ln(1 - e^{-ax})\, dx\right] \qquad \text{(A2)}$$

For $a > 0$, the logarithm can be expanded as a power series in $\exp(-ax)$, which can be integrated term by term:

$$\int \ln(1 - e^{-ax})\, \mathrm{d}x = \int(-e^{-ax} - \tfrac{1}{2}e^{-2ax} - \tfrac{1}{3}e^{-3ax} - \cdots)\mathrm{d}x$$
$$= a^{-1} \sum_{i=1}^{\infty} i^{-2}\, e^{-iax} \qquad \text{(A3)}$$

The final expression for the integral of equation (1) is thus:

$$\frac{1}{2N}[s\ln(1-\ e^{-2N_e s}) - (2N_e)^{-1}\sum_{i=1}^{\infty} i^{-2}\, e^{-2iN_e s}] \qquad \text{(A4)}$$

The contribution to the mean fixation probability from the interval s_i to s_{i+1} is obtained by dividing this expression by ($s_{i+1} - s_i$).

For $s_0 = 0$, equation (A4) is invalid. However, the integral between 0 and a small positive value of s, s_ε, can be found as follows. For $2N_e s << 1$, the initial integrand can be approximated by $a^{-1}(1-ax/2)$, so that equation 2 can be replaced with:

$$a^{-1}x - \frac{1}{4}x^2$$

and the indefinite integral of the fixation probability becomes:

$$[(2N_e)^{-1}s - \frac{1}{4}s^2](N_e/N) = \frac{s}{2N}[1 - \frac{1}{2}N_e s)] \qquad \text{(A5a)}$$

The contribution to the integral of P_{fix} between $s_0 = 0$ and s_1 from the interval $(0, s_\varepsilon)$ is thus:

$$[(2N_e)^{-1}s_\varepsilon - \frac{1}{2}s_\varepsilon^2](N_e/N) = \frac{s_\varepsilon}{2N}[1 - \frac{1}{2}(N_e s_\varepsilon)] \qquad \text{(A5b)}$$

The corresponding mean fixation probability over this interval is:

$$\frac{1}{2N}[1 - \frac{1}{2}s(N_e s_\varepsilon)]$$

This is slightly smaller than the neutral value, $1/(2N)$, as would be expected when $2N_e s << 1$.

Thus, for the interval (s_0, s_1) with $s_0 = 0$, equation (A5b) should be used for the interval $(0 \leq s \leq s_\varepsilon)$, and equation (A4) with integration limits s_ε and s_1 for the remainder of the interval.

FIGURES AND TABLES

Table 1: Reduction in nucleotide diversity at linked neutral sites relative to the neutral value after the fixation of a weakly deleterious or advantageous semi-dominant mutation. The distance between the selected and neutral site is presented in units of the scaled recombination rate (ρ), as well as in the number of bases corresponding to *Drosophila*-like populations.

Distance from selected site in scaled recombination rate (ρ)	**Corresponding number of bases in *Drosophila***		**Expected diversity reduction**	**Expected diversity reduction**		**Expected diversity reduction**	
	Without gene conversion	**With gene conversion**	$\mathbf{2Ns = 0}$	$\mathbf{2Ns = 5}$		$\mathbf{2Ns = 10}$	
				A	**B**	**A**	**B**
0	0	0	0.426	0.459	0.496	0.523	0.534
0.05	2.5	0.8	0.393	0.429	0.471	0.502	0.514
0.10	5	1.7	0.372	0.409	0.446	0.479	0.495
0.20	10	3.3	0.325	0.371	0.402	0.452	0.459
0.40	20	6.7	0.261	0.301	0.328	0.393	0.395
0.80	40	13.5	0.184	0.221	0.228	0.304	0.298
1.60	80	27.2	0.100	0.127	0.138	0.200	0.182
3.20	160	55.6	0.047	0.063	0.100	0.107	0.101
6.40	320	116	0.018	0.025	0.077	0.044	0.069
12.8	640	254	0.006	0.009	0.043	0.014	0.040

The double entries in the two right-hand columns are the results of A) 1000 replicate simulations using equation (27) of Tajima (1990), and B) the analytical approximation of Charlesworth (2020b, equation 14). For the simulations, a population size of 100 and a scaled neutral mutation rate per bp of 2.5 x 10^{-6} were assumed. 1000 replicate runs were performed. Note that if the diffusion approximation is valid, only the scaled parameter values (ρ, $2Ns$ and $\theta = 4Nu = 0.001$) are relevant.

Table 2: Mean genome-wide and outlier F_{ST} values (calculated in windows of 500 bp (labeled 'Constant total sites'), or 10 SNPs (labeled 'Constant SNPs')).

Evolutionary model	**Mean F_{ST}**		**Outlier F_{ST} (1%)**		**Outlier F_{ST} (1%)/ Mean F_{ST}**	
	Constant total sites	Constant SNPs	Constant total sites	Constant SNPs	Constant total sites	Constant SNPs
Neutrality	0.0374	0.0363	0.0874	0.1628	2.3369	4.4838
Purifying selection	0.0365	0.0352	0.0880	0.1454	2.4110	4.1296
Purifying selection (rescaled DFE)	0.0666	0.0613	0.1585	0.2637	2.3799	4.2999
With 1% weak positive selection	0.0578	0.0523	0.1403	0.2412	2.4273	4.6150
With 1% strong positive selection	0.2261	0.1976	0.7673	0.7455	3.3936	3.7731
Neutral values, with the Li & Stephan (2006) bottleneck	0.2828	0.2557	0.4154	0.6956	1.4689	2.7204

These results, with the exception of the Li & Stephan row, use the Arguello *et al.* (2019) parameters for European and African *D. melanogaster* population history, under different DFE configurations. Additional details may be found in the text and Supp Table 10.

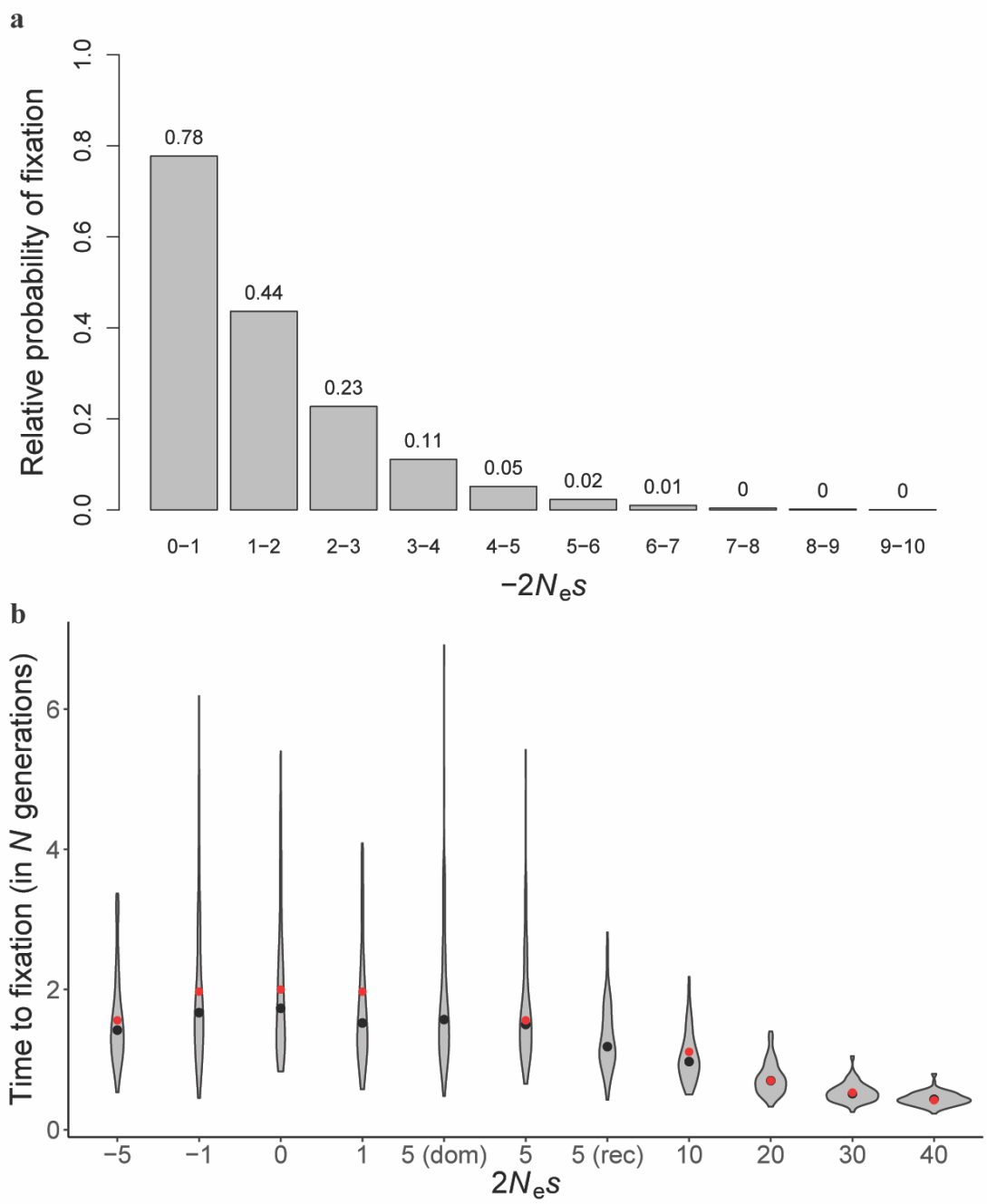

Figure 1: (a) Probability of fixation of weakly deleterious mutations relative to that of neutral mutations. (b) The distribution of fixation times (conditional on fixation) of mutations with varying selective effects, obtained from 100 simulated replicates. Fixation times are measured as the time taken for the mutant allele to spread from frequency $1/2N$ to frequency 1. Black solid circles are the means of the distributions obtained from simulations, and red solid circles are the mean expectations obtained from numerically integrating the expression of Kimura & Ohta (1969). The dominance coefficient is 0.5 for all mutations except in the cases "dom" and "rec" where $h = 1$ and 0, respectively.

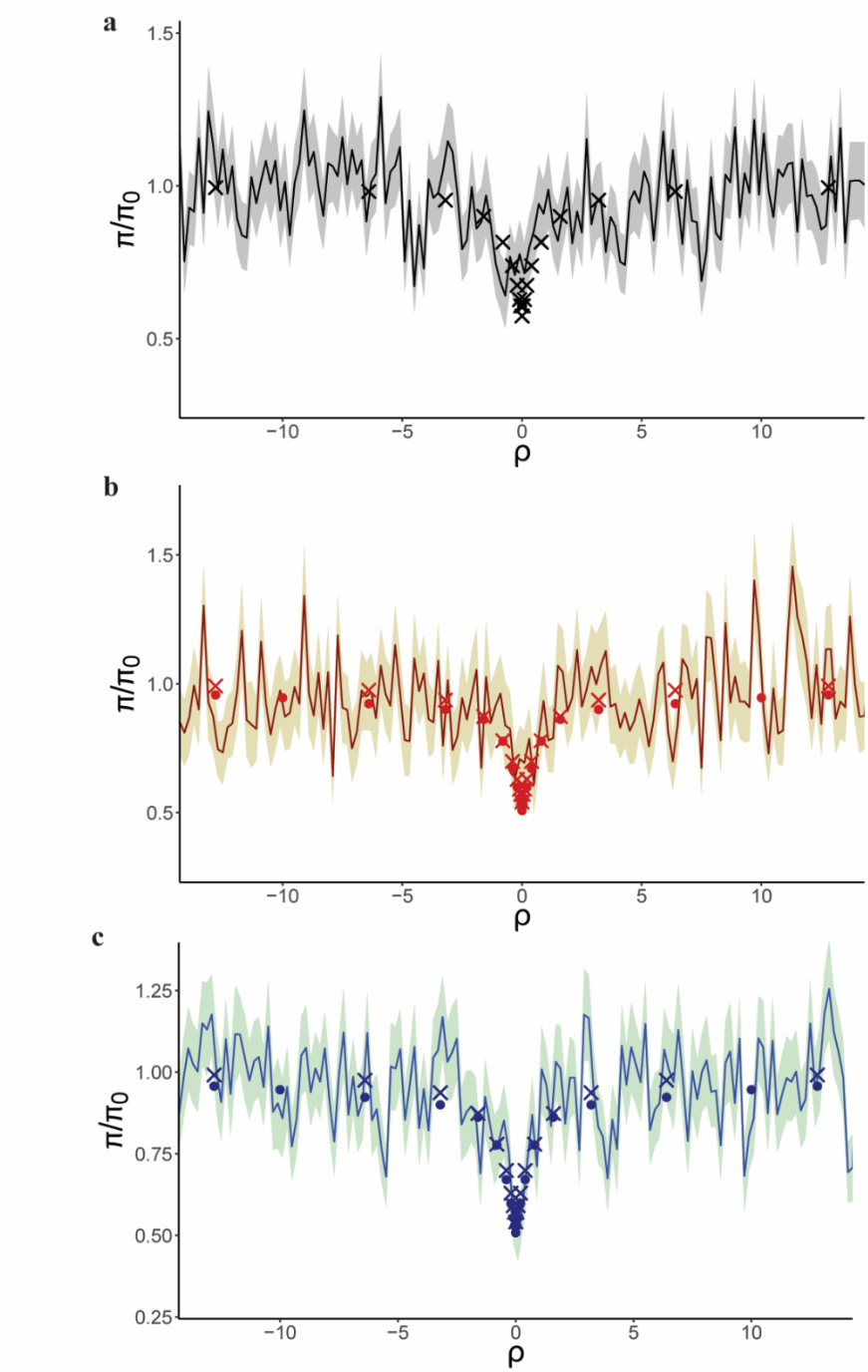

677

678 **Figure 2**: Recovery of nucleotide diversity per site (π) relative to that expected under neutrality
679 (π_0), around a recent fixation (shown at position 0 on the x-axis). The target site has experienced
680 (a) a neutral fixation ($2Ns = 0$; black lines), (b) a weakly deleterious fixation ($2Ns_d = 5$; red
681 line), and (c) a weakly beneficial fixation ($2Ns_a = 5$; blue line). Solid lines represent mean
682 values of 100 replicates, shaded regions correspond to 1 SE above and 1 SE below the mean.
683 Solid circles show the theoretical predictions using equation (14) of Charlesworth 2020b; and
684 crosses correspond to simulations based on equation (27) of Tajima (1990).

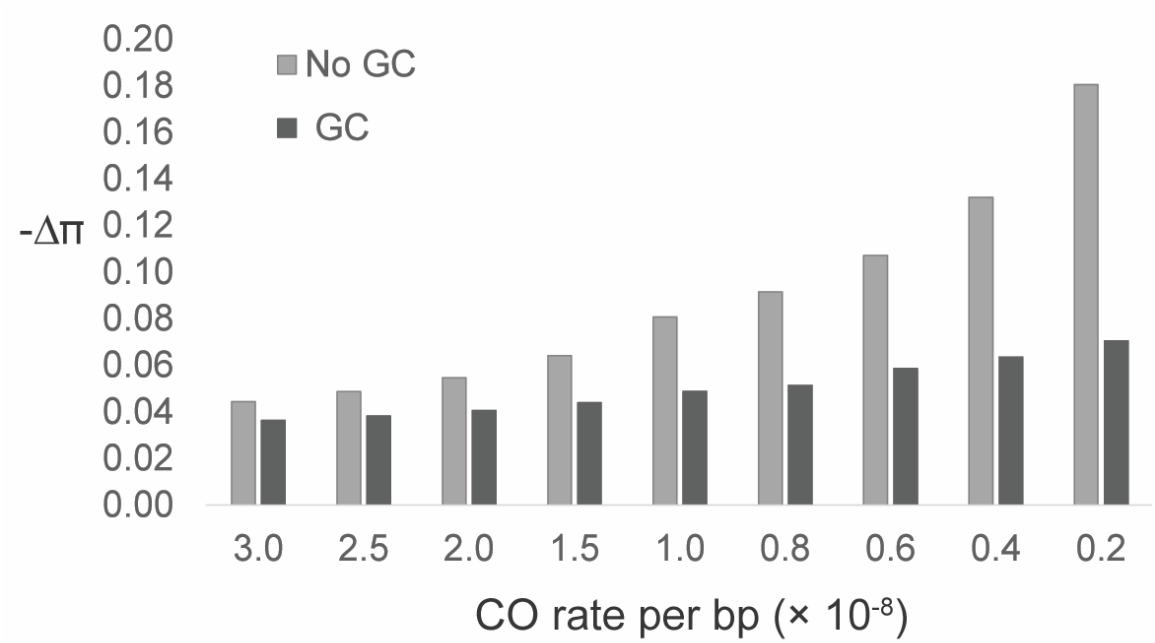

Figure 3: Predicted mean reductions of nucleotide diversity at linked neutral sites compared to neutrality ($-\Delta\pi$), due to the recurrent fixation of weakly deleterious semi-dominant mutations with $2.5 \leq 2Ns_d \leq 10$. Nucleotide diversity at neutral sites was averaged across a gene comprised of five 300-bp exons and 100-bp introns, in which all intronic sites and 30% of exonic sites were neutral.

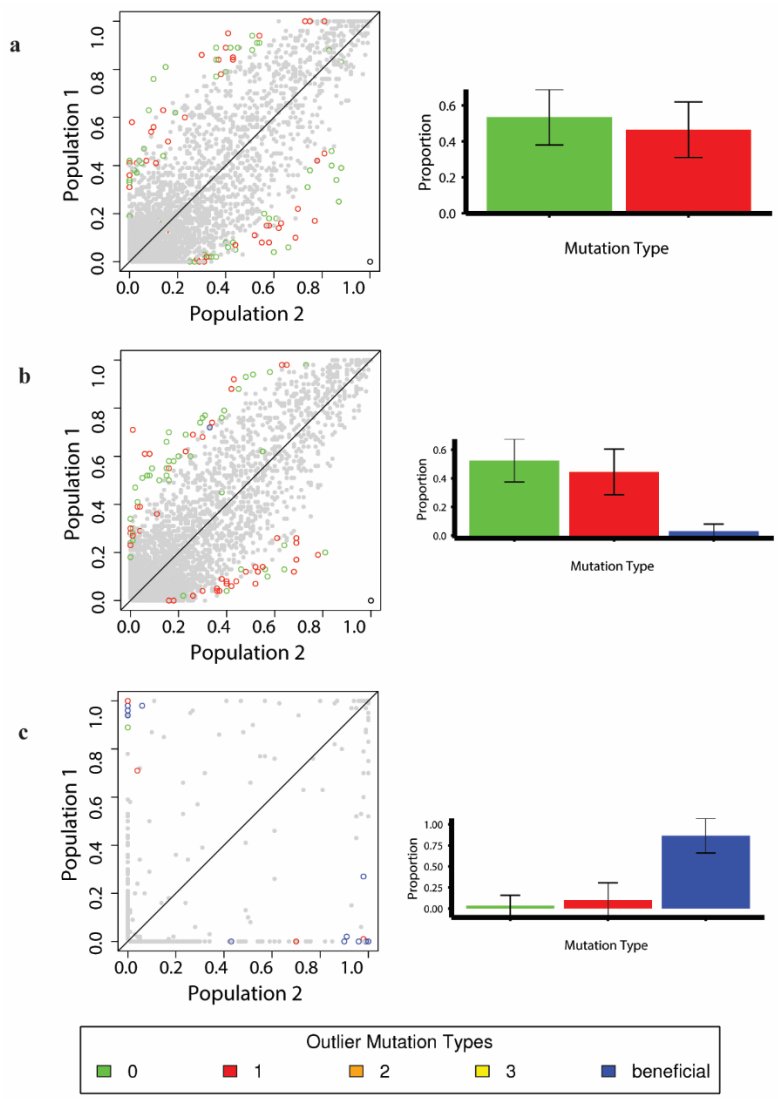

Figure 4: Allele frequencies of SNPs in simulated population 1 (European) *vs* population 2 (African), using parameters of the Arguello *et al.* (2019) model, where the selective effects of all mutations were rescaled with respect to their population sizes after the split (*i.e.,* keeping the strength of selection constant in both populations). Genomic elements experienced (a) purifying selection following the DFE inferred by Johri *et al.* (2020); (b) the same DFE, but with the addition of 1% beneficial mutations with selective effects between $1 < 2Ns_a \leq 10$; or (c) the same DFE, but with the addition of 1% beneficial mutations with selective effects of $2Ns_a = 1000$. *Left panel*: Allele frequency plots for 10 (out of 100) replicates simulated. Colored open circles represent F_{ST} outliers. Green depicts effectively neutral mutations (belonging to class 0), blue depicts beneficial mutations, and warm colors depict deleterious mutations (belonging to classes 1, 2, and 3), with red representing weakly deleterious mutations. *Right panel*: The distribution of fitness effects of outlier mutations for the corresponding scenarios, showing the mean and standard deviation for all 100 replicates. Sites that were fixed in both populations for the same allele were not included in this analysis.

710 **CITATIONS**

711 Andolfatto P., 2005 Adaptive evolution of non-coding DNA in *Drosophila*. Nature 437: 1149-
712 1152.

713 Andolfatto P., 2007 Hitchhiking effects of recurrent beneficial amino acid substitutions in the
714 *Drosophila melanogaster* genome. Genome Res. 17: 1755–1762.

715 Arguello J.R., S. Laurent, and A.G. Clark, 2019 Demographic history of the human commensal
716 *Drosophila melanogaster*. Genome Biol. Evol. 11: 844–854.
717
718 Atkinson, K.E., 1989 Introduction to numerical analysis. John Wiley, New York, NY.
719
720 Bank, C., M. Foll, A. Ferrer-Admetlla, G. Ewing, and J.D. Jensen, 2014a Thinking too positive?
721 Revisiting current methods in population genetic selection inference. Trends Genet. 30: 540-6.
722
723 Bank C., R.T. Hietpas, A. Wong, D.N. Bolon, and J.D. Jensen, 2014b A Bayesian MCMC
724 approach to assess the complete distribution of fitness effects of new mutations: uncovering the
725 potential for adaptive walks in challenging environments. Genetics 196: 841–852.
726
727 Barton N.H., 2000 Genetic hitchhiking. Phil. Trans. R. Soc. Lond. B 355: 1553-62.
728
729 Campos J.L., L. Zhao, and B. Charlesworth, 2017 Estimating the parameters of background
730 selection and selective sweeps in *Drosophila* in the presence of gene conversion. Proc. Natl.
731 Acad. Sci. U.S.A. 114: E4762–E4771.
732
733 Campos J.L., and B. Charlesworth, 2019 The effects on neutral variability of recurrent selective
734 sweeps and background selection. Genetics 212: 287–303.
735
736 Charlesworth B., M.T. Morgan, and D. Charlesworth, 1993 The effect of deleterious mutations
737 on neutral molecular variation. Genetics 134: 1289–1303.
738
739 Charlesworth B., 2020a How long does it take to fix a favorable mutation, and why should we
740 care? Am. Nat. 195: 753–771.
741
742 Charlesworth B., 2020b How good are predictions of the effects of selective sweeps on levels of
743 neutral diversity? bioRxiv 2020.05.27.119883.
744
745 Charlesworth J., and A. Eyre-Walker, 2007 The other side of the nearly neutral theory, evidence
746 of slightly advantageous back-mutations. Proc. Natl. Acad. Sci. USA 104: 16992-997.
747
748 Charlesworth J., and A. Eyre-Walker, 2008 The McDonald–Kreitman test and slightly
749 deleterious mutations. Mol. Biol. Evol. 25: 1007–1015.
750
751 Comeron J.M., R. Ratnappan, and S. Bailin, 2012 The many landscapes of recombination in
752 *Drosophila melanogaster*. PLoS Genet. 8:e1002905.

753
754 Crisci J., Y.-P. Poh, S. Mahajan, and J.D. Jensen, 2013 The impact of equilibrium assumptions
755 on tests of selection. Front. Genet. 4: 235.
756
757 Crow J.F., 1993 Mutation, mean fitness, and genetic load. Oxf. Surv. Evol. Biol. 9: 3-42.
758
759 Cruickshank T.E., and M.W. Hahn, 2014 Reanalysis suggests that genomic islands of speciation
760 are due to reduced diversity, not reduced gene flow. Mol. Ecol. 23: 3133–3157.
761
762 Elyashiv E., S. Sattath, T.T. Hu, A. Strutsovsky, G. McVicker, et al., 2016 A genomic map of the
763 effects of linked selection in *Drosophila*. PLoS Genet. 12: e1006130.
764
765 Eyre-Walker A., and P.D. Keightley, 2007 The distribution of fitness effects of new mutations.
766 Nat. Rev. Genet. 8: 610-8.
767
768 Eyre-Walker A., and P.D. Keightley, 2009 Estimating the rate of adaptive molecular evolution in
769 the presence of slightly deleterious mutations and population size change. Mol. Biol. Evol. 26:
770 2097–2108.
771
772 Fay J., G.J. Wycoff, and C.-I Wu, 2001 Positive and negative selection on the human genome.
773 Genetics 158: 1227-1234
774
775 Fay J., G.J. Wycoff, and C.-I Wu, 2002 Testing the neutral theory of molecular evolution with
776 genomic data from *Drosophila*. Nature 415: 1024-1026.
777
778 Fisher R.A. 1922. On the dominance ratio. Proceedings of the Royal Society of Edinburgh 42:
779 321-341.

780 Fisher R.A., 1930 *The genetical theory of natural selection*. Clarendon Press, Oxford.

781 Fiston-Lavier A.-S., N.D. Singh, M. Lipatov, and D.A. Petrov, 2010 *Drosophila melanogaster*
782 recombination rate calculator. Gene 463: 18–20.

783 Frisse L., R.R. Hudson, A. Bartoszewicz, J.D. Wall, J. Donfack, and A. Di Rienzo, 2001 Gene
784 conversion and population histories may explain the contrast between polymorphism and linkage
785 disequilibrium levels. Am. J. Hum. Genet. 69: 831-43.

786 Gillespie J.H., 1994 Substitution processes in molecular evolution. III. Deleterious alleles.
787 Genetics 138: 943-952.

788 Glinka S.L., L. Ometto, S. Mousset, W. Stephan, and D. De Lorenzo, 2003 Demography and
789 natural selection have shaped genetic variation in *Drosophila melanogaster*: a multi-locus
790 approach. Genetics 165:1269–1278.

Haddrill P.R., K.R. Thornton, B. Charlesworth, and P. Andolfatto, 2005 Multilocus patterns of nucleotide variability and the demographic and selection history of *Drosophila melanogaster* populations. Genome Res. 15:790–799.

Haldane J.B.S. 1927. A mathematical theory of natural and artificial selection. Part V. Selection and mutation. Math. Proc. Camb. Philos. Soc 23:838-844.

Haller B.C., and P.W. Messer, 2017 asymptoticMK: A web-based tool for the asymptotic McDonald–Kreitman test. G3 7: 1569–1575.

Haller B.C., and P.W. Messer, 2019 SLiM 3: Forward genetic simulations beyond the Wright-Fisher model. Mol. Biol. Evol. 36: 632–637.

Halligan D.L., and P.D. Keightley, 2006 Ubiquitous selective constraints in the *Drosophila* genome revealed by a genome-wide interspecies comparison. Genome Res. 16: 875–884.

Harr B., M. Kauer, and C. Schlotterer, 2002 Hitchhiking mapping: a population-based fine-mapping strategy for adaptive mutations in *Drosophila melanogaster*. Proc. Natl. Acad. Sci. USA 99: 12949–12954.

Harris R.B., A. Sackman, and J.D. Jensen, 2018 On the unfounded enthusiasm for soft selective sweeps II: examining recent evidence from humans, flies, and viruses. PLoS Genetics 14(12): e1007859.

Hartfield M., and T. Bataillon, 2020 Selective sweeps under dominance and inbreeding. G3 10: 1063-75.

Hernandez R.D., J.L. Kelley, E. Elyashiv, S.C. Melton, A. Auton, et al., 2011 Classic selective sweeps were rare in recent human evolution. Science 331: 920–924.

Hudson R.R., M. Slatkin, and W.P. Maddison, 1992 Estimating levels of gene flow from DNA sequence data. Genetics 13: 583-589.

Jacquier H., A. Birgy, H.L. Nagard, Y. Mechulam, E. Schmitt, et al., 2013 Capturing the mutational landscape of the beta-lactamase TEM-1. Proc. Natl. Acad. Sci. USA 110: 13067–13072.

Jakobsson M., M.D. Edge, and N.A. Rosenberg, 2013 The relationship between F_{ST} and the frequency of the most frequent allele. Genetics 193: 515–528.

Jensen J.D., Y. Kim, V.B. DuMont, C.F. Aquadro, and C.D. Bustamante, 2005 Distinguishing between selective sweeps and demography using DNA polymorphism data. Genetics 170:1401–1410.

Jensen J.D., K.R. Thornton, and P. Andolfatto, 2008 An approximate Bayesian estimator suggests strong recurrent selective sweeps in *Drosophila*. PLoS Genet. 4:e1000198.

832 Jensen J.D., 2009 On reconciling single and recurrent hitchhiking models. Genome Biol. Evol. 1:
833 320-4.
834
835 Johri P., B. Charlesworth, and J.D. Jensen, 2020 Toward an evolutionarily appropriate null
836 model: jointly inferring demography and purifying selection. Genetics 215: 173–192.
837
838 Keightley P.D., U. Trivedi, M. Thomson, F. Oliver, S. Kumar, et al., 2009 Analysis of the
839 genome sequences of three *Drosophila melanogaster* spontaneous mutation accumulation lines.
840 Genome Res. 19: 1195–1201.
841
842 Keightley P.D., R.W. Ness, D.L. Halligan, and P.R. Haddrill, 2014 Estimation of the
843 spontaneous mutation rate per nucleotide site in a *Drosophila melanogaster* full-sib family.
844 Genetics 196: 313–320.

845 Kim Y., 2006 Allele frequency distribution under recurrent selective sweeps. Genetics 172:
846 1967–1978.

847 Kim Y., and W. Stephan, 2002 Detecting a local signature of genetic hitchhiking along a
848 recombining chromosome. Genetics 160: 765–777.

849 Kimura M., 1957 Some problems of stochastic processes in genetics. Ann. Math. Stat. 28: 882-
850 901.
851
852 Kimura M., 1962 On the probability of fixation of mutant genes in a population. Genetics 47:
853 713–719.
854
855 Kimura M., 1964 Diffusion models in population genetics. J. Appl. Probab. 1: 177-232.
856
857 Kimura, M., 1970 The length of time required for a selectively neutral mutation to reach fixation
858 through random frequency drift in a finite population. Genet. Res. 15: 131-133.
859
860 Kimura M., and T. Ohta, 1969 The average number of generations until fixation of a mutant gene
861 in a finite population. Genetics 61: 763–771.
862
863 Li H., and W. Stephan, 2006 Inferring the demographic history and rate of adaptive substitution
864 in *Drosophila*. PLoS Genet. 2: e166.
865
866 Li Y.J., Y. Satta, and N. Takahata, 1999 Paleo-demography of the *Drosophila melanogaster*
867 subgroup: application of the maximum likelihood method. Genes Genet. Syst. 74: 117–127.
868
869 Lynch M., D. Blanchard, D. Houle, T. Kibota, S. Schultz, L. Vassilieva, and J. Willis, 1999
870 Spontaneous deleterious mutations. Evolution 53: 645-63.

871 Macpherson J.M., G. Sella, J.C. Davis, and D.A. Petrov, 2007 Genome-wide spatial
872 correspondence between nonsynonymous divergence and neutral polymorphism reveals
873 extensive adaptation in *Drosophila*. Genetics 177: 2083–2099.

Mafessoni F., and M. Lachmann, 2015 Selective strolls: fixation and extinction in diploids are slower for weakly selected mutations than for neutral ones. Genetics 201: 1581-1589.

Maruyama T., and M. Kimura, 1974 A note on the speed of gene frequency changes in reverse directions in a finite population. Evolution 28: 161-163.

Maynard Smith J., and J. Haigh, 1974 The hitch-hiking effect of a favourable gene. Genet. Res. 23: 23-35.

McDonald J.H., and M. Kreitman, 1991 Adaptive protein evolution at the Adh locus in *Drosophila*. Nature 351:652–654.

Messer P.W., and D.A. Petrov, 2013 Frequent adaptation and the McDonald–Kreitman test. Proc. Natl. Acad. Sci. U.S.A. 110: 8615–8620.

Miller D.E., C.B. Smith, N.Y. Kazemi, A.J. Cockrell, A.V. Arvanitakis, J.P. Blumenstiel, S.L. Jaspersen, and R.S. Hawley, 2016 Whole-genome analysis of individual meiotic events in *Drosophila melanogaster* reveals that noncrossover gene conversions are insensitive to interference and the centromere effect. Genetics 203:159–171.

Nielsen R., S. Williamson, Y. Kim, M.J. Hubisz, A.G. Clark, and C.D. Bustamante, 2005 Genomics scans for selective sweeps using SNP data. Genome Res. 15: 1566–1575.

Pavlidis P., J.D. Jensen, W. Stephan, and A. Stamatakis, 2012 A critical assessment of storytelling: Gene Ontology categories and the importance of validating genomic scans. Mol. Biol. Evol. 29: 3237–3248.

Pfeifer B., U. Wittelsbürger, S.E. Ramos-Onsins, and M.J. Lercher, 2014 PopGenome: an efficient Swiss army knife for population genomic analyses in R. Mol. Biol. Evol. 31: 1929–1936.

Przeworski M., 2002 The signature of positive selection at randomly chosen loci. Genetics 160: 1179–1189.

R Core Team, 2018 R: A language and environment for statistical computing. R Foundation for Statistical Computing, Vienna, Austria. URL https://www.R-project.org/.

Sanjuán R., 2010 Mutational fitness effects in RNA and single-stranded DNA viruses: common patterns revealed by site-directed mutagenesis studies. Philos. Trans. R. Soc. Lond. B Biol. Sci. 365: 1975-82.

Sattath S., E. Elyashiv, O. Kolodny, Y. Rinott, and G. Sella, 2011 Pervasive adaptive protein evolution apparent in diversity patterns around amino acid substitutions in *Drosophila simulans*. PLoS Genet. 7:e1001302.

910 Sella G., D.A. Petrov, M. Przeworski, and P. Andolfatto, 2009 Pervasive natural selection in the
911 Drosophila genome. PLoS Genet. 5:e1000495.

912 Stephan W., 2019 Selective sweeps. Genetics 211: 5-13.

913 Tajima F., 1990 Relationship between DNA polymorphism and fixation time. Genetics 125:
914 447–454.

915 Teshima K.M., G. Coop, and M. Przeworski, 2006 How reliable are empirical genome scans for
916 selective sweeps? Genome Res. 16: 702–712.

917 Thornton K., 2003 Libsequence: a C++ class library for evolutionary genetic analysis.
918 Bioinformatics 19: 2325–2327.
919
920 Thornton K.R., and J.D. Jensen, 2007 Controlling the false positive rate in multi-locus genome
921 scans for selection. Genetics 175: 737-750.

922 Wiehe T.H., and W. Stephan, 1993 Analysis of a genetic hitchhiking model and its application to
923 DNA polymorphism data from *Drosophila melanogaster*. Mol. Biol. Evol. 10: 842–854.

924 Wright S., 1931 Evolution in Mendelian populations. Genetics 16:97-159.

925

926

927

928

929

930

931

932

933

934

935

936

937

938

939 **SUPPLEMENTARY MATERIAL**

940 **Supp Table 1**: Parameters of the demographic models of *D. melanogaster* simulated for the F_{ST}
941 analyses.

	Arguello *et al.* 2019	**Li & Stephan 2006**
Ancestral population size	1.95×10^6	8.603×10^6
Time of split of European population	6.62×10^4 generations ago	1.58×10^5 generations ago
European bottleneck size	-	2.2×10^3
European bottleneck duration	-	3.4×10^3 generations
European current size	4.73×10^5	1.075×10^6
African current size	3.91×10^6	8.603×10^6

942

943

944

945 **Supp Table 2**: The means and standard deviations of fixation times (conditional on fixation) of
946 mutations with varying selective effects, obtained from 100 simulated replicates. Fixation times
947 are measured as the time taken for the mutant allele to spread from frequency $1/2N$ to frequency
948 1. Unless otherwise indicated, h=0.5.
949

	Time to fixation (in $2N$ generations)						
$2Ns$	**min**	**First quartile (25%)**	**Median (50%)**	**Mean**	**Max**	**SD**	**Analytical Mean**
0	0.57	1.30	1.82	2.08	5.77	1.04	2.00
-1	0.45	1.20	1.67	1.96	6.19	1.05	1.97
1	0.58	1.14	1.52	1.73	4.09	0.99	1.97
-5	0.53	1.14	1.36	1.55	3.37	0.74	1.56
5	0.58	1.15	1.49	1.66	5.42	0.57	1.56
5 (h=0)	0.43	0.99	1.19	1.31	2.82	0.47	-
5 (h=1)	0.49	1.21	1.57	1.83	6.91	0.99	-
10	0.50	0.77	0.97	1.04	2.18	0.36	1.11
20	0.33	0.56	0.70	0.73	1.40	0.23	0.70
30	0.25	0.44	0.51	0.53	1.05	0.14	0.53
40	0.23	0.38	0.43	0.44	0.80	0.10	0.42

Supp Table 3: Reduction in diversity (relative to a value of 1 for neutrality) as (A) obtained by Tajima's (1990) simulations and (B) as approximated by numerical results using equation (14) in Charlesworth 2020b.

	$2Ns_a = 4$		$2Ns_a = 8$		$2Ns_a = 20$		$2Ns_a = 40$		$2Ns_a = 80$	
ρ	**A**	**B**	**A**	**B**	**A**	**B**	**A**	**B**	**A**	**B**
0	0.448	0.513	0.494	0.512	0.620	0.633	0.734	0.741	0.830	0.830
0.005	0.445	0.511	0.492	0.510	0.619	0.632	0.732	0.740	0.830	0.830
0.05	0.422	0.486	0.473	0.490	0.606	0.618	0.723	0.730	0.823	0.824
0.10	0.398	0.461	0.453	0.469	0.592	0.604	0.713	0.720	0.816	0.817
0.25	0.398	0.417	0.401	0.412	0.552	0.563	0.684	0.690	0.796	0.796
0.50	0.266	0.306	0.333	0.335	0.493	0.501	0.638	0.643	0.763	0.764
1.00	0.179	0.201	0.240	0.229	0.399	0.399	0.558	0.559	0.702	0.702
2.50	0.077	0.114	0.114	0.111	0.231	0.215	0.384	0.372	0.550	0.548
5.00	0.031	0.093	0.049	0.079	0.113	0.102	0.222	0.201	0.375	0.368
10.0	0.010	0.057	0.016	0.051	0.041	0.053	0.113	0.080	0.190	0.177

Supp Table 4: Reduction of diversity ($\Delta\pi$) at ρ ($= 4Nr$) distance from the selected site for varying dominance (h) and selection coefficients ($2Ns$) calculated using the algorithm presented in Tajima (1990). For the purpose of these calculations N was assumed to be 100 and $\theta = 0.001$.

		ρ									
	$\Delta\pi$	**0**	**0.05**	**0.1**	**0.2**	**0.4**	**0.8**	**1.6**	**3.2**	**6.4**	**12.8**
$2Ns = 0$; 100000 replicates											
	Mean	0.4215	0.3907	0.3635	0.3178	0.2508	0.1706	0.0966	0.0451	0.0178	0.0062
	SE	3.3E-04	3.5E-04	3.6E-04	3.8E-04	3.9E-04	3.6E-04	2.7E-04	1.6E-04	7.1E-05	2.4E-05
$2Ns_a = 2$ [$2Ns_d = 2$]; 100000 replicates											
***h*=0**	**Mean**	0.4430	0.4157	0.3909	0.3482	0.2825	0.1990	0.1164	0.0556	0.0220	0.0076
[*h*=1]	**SE**	3.3E-04	3.4E-04	3.5E-04	3.7E-04	3.8E-04	3.5E-04	2.7E-04	1.6E-04	7.6E-05	3.1E-05
***h*=0.1**	**Mean**	0.4400	0.4121	0.3871	0.3440	0.2781	0.1949	0.1149	0.0547	0.0217	0.0075
[*h*=0.9]	**SE**	3.3E-04	3.4E-04	3.6E-04	3.7E-04	3.8E-04	3.5E-04	2.7E-04	1.6E-04	7.4E-05	3.0E-05
***h*=0.2**	**Mean**	0.4371	0.4089	0.3836	0.3401	0.2741	0.1913	0.1109	0.0527	0.0208	0.0072
[*h*=0.8]	**SE**	3.3E-04	3.5E-04	3.6E-04	3.7E-04	3.8E-04	3.5E-04	2.7E-04	1.6E-04	7.4E-05	2.7E-05
***h*=0.3**	**Mean**	0.4344	0.4057	0.3801	0.3364	0.2704	0.1880	0.1085	0.0514	0.0203	0.0070
[*h*=0.7]	**SE**	3.3E-04	3.5E-04	3.6E-04	3.8E-04	3.8E-04	3.5E-04	2.7E-04	1.6E-04	7.4E-05	2.9E-05
***h*=0.4**	**Mean**	0.4317	0.4029	0.3769	0.3328	0.2664	0.1843	0.1061	0.0501	0.0198	0.0069
[*h*=0.6]	**SE**	3.3E-04	3.5E-04	3.6E-04	3.8E-04	3.9E-04	3.5E-04	2.7E-04	1.6E-04	7.3E-05	2.9E-05
***h*=0.5**	**Mean**	0.4289	0.3996	0.3734	0.3290	0.2623	0.1807	0.1035	0.0488	0.0192	0.0067
[*h*=0.5]	**SE**	3.3E-04	3.5E-04	3.6E-04	3.8E-04	3.9E-04	3.5E-04	2.7E-04	1.6E-04	7.2E-05	2.6E-05
***h*=0.6**	**Mean**	0.4264	0.3967	0.3699	0.3251	0.2585	0.1773	0.1011	0.0474	0.0187	0.0065
[*h*=0.4]	**SE**	3.3E-04	3.5E-04	3.6E-04	3.8E-04	3.9E-04	3.5E-04	2.7E-04	1.6E-04	7.2E-05	2.8E+00
***h*=0.7**	**Mean**	0.4236	0.3935	0.3665	0.3210	0.2545	0.1737	0.0987	0.0461	0.0182	0.0064
[*h*=0.3]	**SE**	3.3E-04	3.5E-04	3.6E-04	3.8E-04	3.9E-04	3.5E-04	2.6E-04	1.5E-04	7.1E-05	2.8E-05
***h*=0.8**	**Mean**	0.4211	0.4032	0.3769	0.3326	0.2673	0.1896	0.0963	0.0449	0.0177	0.0062
[*h*=0.2]	**SE**	3.3E-04	3.3E-04	3.5E-04	3.6E-04	3.7E-04	3.3E-04	2.6E-04	1.5E-04	7.1E-05	3.1E-05
***h*=0.9**	**Mean**	0.4218	0.3868	0.3595	0.3132	0.2463	0.1666	0.0938	0.0436	0.0171	0.0060
[*h*=0.1]	**SE**	3.4E-04	3.5E-04	3.6E-04	3.8E-04	3.9E-04	3.5E-04	2.6E-04	1.5E-04	7.1E-05	3.0E-05
***h*=1**	**Mean**	0.4158	0.3842	0.3562	0.3097	0.2429	0.1633	0.0915	0.0425	0.0167	0.0059
[*h*=0]	**SE**	3.3E-04	3.5E-04	3.7E-04	3.8E-04	3.9E-04	3.5E-04	2.6E-04	1.5E-04	7.1E-05	2.7E-05
$2Ns_a = 5$ [$2Ns_d = 5$]; 1000 replicates											
***h*=0**	**Mean**	0.4916	0.4724	0.4422	0.4006	0.3516	0.2554	0.1544	0.0812	0.0321	0.0109
[*h*=1]	**SE**	3.1E-03	3.2E-03	3.3E-03	3.3E-03	3.6E-03	3.4E-03	2.8E-03	1.8E-03	8.2E-04	3.1E-04
***h*=0.9**	**Mean**	0.4249	0.4022	0.3755	0.3357	0.2712	0.1899	0.1119	0.0523	0.0213	0.0074
[*h*=0.1]	**SE**	3.5E-03	3.7E-03	3.7E-03	4.0E-03	4.1E-03	3.7E-03	2.7E-03	1.7E-03	7.9E-04	3.0E-04
***h*=1**	**Mean**	0.4201	0.3932	0.3717	0.3268	0.2677	0.1774	0.1046	0.0530	0.0185	0.0068
[*h*=0]	**SE**	3.5E-04	3.5E-03	3.9E-03	3.9E-03	4.2E-03	3.7E-03	2.8E-03	1.7E-03	7.7E-04	3.0E-04
$2Ns_a = 10$ [$2Ns_d = 10$]; 1000 replicates											
***h*=0**	**Mean**	0.5701	0.4724	0.4422	0.4006	0.3516	0.2554	0.1544	0.0812	0.0321	0.0109
[*h*=1]	**SE**	2.5E-03	3.2E-03	3.3E-03	3.3E-03	3.6E-03	3.4E-03	2.8E-03	1.8E-03	8.2E-04	3.1E-04
***h*=1**	**Mean**	0.4507	0.4315	0.4124	0.3796	0.3231	0.2452	0.1548	0.0794	0.0319	0.0109
[*h*=0]	**SE**	1.2E-03	1.2E-03	1.2E-03	1.3E-03	1.3E-03	1.2E-03	9.8E-04	6.1E-04	2.9E-04	1.1E-04

Supp Table 5: Distortion of the SFS at neutral sites linked to the selected site at a distance measured by ρ, and calculated immediately after the fixation of a weakly selected mutation. 100 replicates were used to obtain these values. Tajima's *D* was calculated in non-overlapping sliding windows of 50 base pairs, with the distance from the selected site corresponding to the mid-point of the window.

		$2Ns = 0$		$2Ns = +5$		$2Ns = -5$	
ρ	**Number of bases from the selected site in *Drosophila***	Tajima's *D* mean	Tajima's *D* SE	Tajima's *D* mean	Tajima's *D* SE	Tajima's *D* mean	Tajima's *D* SE
1	25	-0.1493	0.0712	-0.2097	0.0671	-0.1852	0.0867
3	75	-0.0979	0.0696	-0.0827	0.0717	-0.0476	0.0919
5	125	0.00165	0.0731	-0.1042	0.0712	-0.0176	0.0871
7	175	-0.0355	0.0657	-0.0731	0.0699	-0.0193	0.0869
9	225	-0.0864	0.0712	-0.0214	0.0729	-0.1359	0.0816

Supp Table 6: Number of polymorphic (*P*) and fixed (*D*) sites at nonsynonymous (*N*) and synonymous (*S*) sites, and the estimated proportion of substitutions fixed by positive selection (α), for an increasing proportion of mildly deleterious mutations at nonsynonymous sites. The ratio of the rate of divergence at nonsynonymous relative to that at synonymous sites is denoted by d_N/d_S.

	% weakly deleterious NS sites	P_N	D_N	P_S	D_S	d_N/d_S	α	α_{asym} **[95% CI]**
Neutral	0%	522	439	255	221	0.99	-0.05	-0.06 [-0.21, 0.09]
Weakly deleterious	50%	447	261	240	237	0.55	-0.58	-0.35 [-0.72, 0.03]
Johri *et al.* DFE	66%	281	60	173	254	0.12	-5.22	-3.55 [-5.10, -2.01]

1030 **Supp Table 7**: Composition of shared and private SNPs between populations (calculated in
1031 sliding windows of 500 bp).
1032

	Fraction of shared SNPs	Fraction of private SNPs in African population	Fraction of private SNPs in European population	Fraction of fixed differences
Neutral	0.538	0.355	0.108	0.000
Purifying selection (rescaled)	0.363	0.521	0.116	0.000
Purifying selection (not rescaled)	0.417	0.440	0.143	0.000
Weak positive selection	0.379	0.502	0.119	0.000
Strong positive selection	0.040	0.640	0.319	0.001
Neutral bottleneck	0.242	0.706	0.052	0.000

1033
1034
1035
1036
1037
1038
1039
1040
1041
1042
1043
1044
1045
1046
1047
1048

1049 **Supp Table 8**: Mean F_{ST} and nucleotide diversity in the African and European population, for
1050 neutral, weakly deleterious, and beneficial mutations separately, calculated for windows of 500
1051 bp.

Mutation type	Model	F_{ST}		Nucleotide diversity			
		Mean	SD	AFR (Mean)	AFR (SD)	EUR (Mean)	EUR (SD)
Neutral	**Neutral**	0.0374	0.0226	0.0317	0.0070	0.0298	0.0071
	Purifying selection (rescaled)	0.0689	0.0556	0.0056	0.0022	0.0046	0.0021
	Purifying selection (not rescaled)	0.0363	0.0276	0.0057	0.0021	0.0054	0.0021
	Weak positive selection	0.0594	0.0479	0.0055	0.0022	0.0047	0.0021
	Strong positive selection	0.1065	0.1815	0.0002	0.0002	0.0002	0.0002
	Neutral bottleneck	0.2828	0.0762	0.1392	0.0145	0.0633	0.0219
Weakly deleterious	**Purifying selection (rescaled)**	0.0621	0.0457	0.0062	0.0021	0.0045	0.0019
	Purifying selection (not rescaled)	0.0361	0.0245	0.0063	0.0021	0.0059	0.0021
	Weak positive selection	0.0540	0.0369	0.0062	0.0021	0.0045	0.0020
	Strong positive selection	0.1489	0.2059	0.0004	0.0003	0.0003	0.0003
Beneficial	**Weak positive selection**	0.0385	0.0616	0.0004	0.0005	0.0004	0.0005
	Strong positive selection	0.3139	0.2952	0.0004	0.0003	0.0002	0.0003

1052

1053

1054

1055

1056

1057

1058

1059 **Supp Table 9**: Average nucleotide diversity (π) per site of African and European populations
1060 simulated for F_{ST} analyses.

Model	Population	π	
		Mean	Standard deviation
Neutral	African	0.1618	0.0086
	European	0.1538	0.0094
Weak positive selection	African	0.1416	0.0062
	European	0.1175	0.0161
Strong positive selection	African	0.0378	0.0128
	European	0.0281	0.0104
Purifying selection (DFE rescaled)	African	0.1131	0.0060
	European	0.0869	0.0095
Purifying selection (DFE not rescaled)	African	0.1079	0.0050
	European	0.0997	0.0054
Neutral bottleneck	African	0.1851	0.0026
	European	0.0841	0.0159

1061

1062

1063

1064

1065

1066

1067

1068

1069

1070

1071

1072

1073

1074 **Supp Table 10**: Mean genome-wide and outlier F_{ST} values for European and African *D.*
1075 *melanogaster* populations (expanded from Table 2) - for window sizes of both 10 and 20 SNPs,
1076 and the 1% and 2.5% tails of the distribution.

Evolutionary model	**Window size**	**Mean F_{ST}**	**Outlier F_{ST} (2.5%)**	**Outlier F_{ST} (1%)**	**Outlier F_{ST} (2.5%) / Mean F_{ST}**	**Outlier F_{ST} (1%) / Mean F_{ST}**
Neutral	10 SNPs	0.0363	0.1585	0.1628	4.3662	4.4838
	20 SNPs	0.0369	0.1411	0.1471	3.8203	3.9844
Purifying selection (rescaled DFE)	10 SNPs	0.0613	0.2497	0.2637	4.0707	4.2999
	20 SNPs	0.0646	0.2234	0.2234	3.4564	3.4564
Purifying selection	10 SNPs	0.0352	0.1467	0.1454	4.1673	4.1296
	20 SNPs	0.0361	0.1311	0.1311	3.6288	3.6288
Neutral bottleneck	10 SNPs	0.2557	0.6459	0.6956	2.5260	2.7204
	20 SNPs	0.2681	0.6071	0.6560	2.2650	2.4472
With weak positive selection	10 SNPs	0.0523	0.2256	0.2412	4.3154	4.6150
	20 SNPs	0.0556	0.1977	0.1977	3.5525	3.5525
With strong positive selection	10 SNPs	0.1976	0.7455	0.7455	3.7731	3.7731
	20 SNPs	0.2617	0.6498	0.6498	2.4832	2.4832

1077

1078

1079

1080

1081

1082

1083

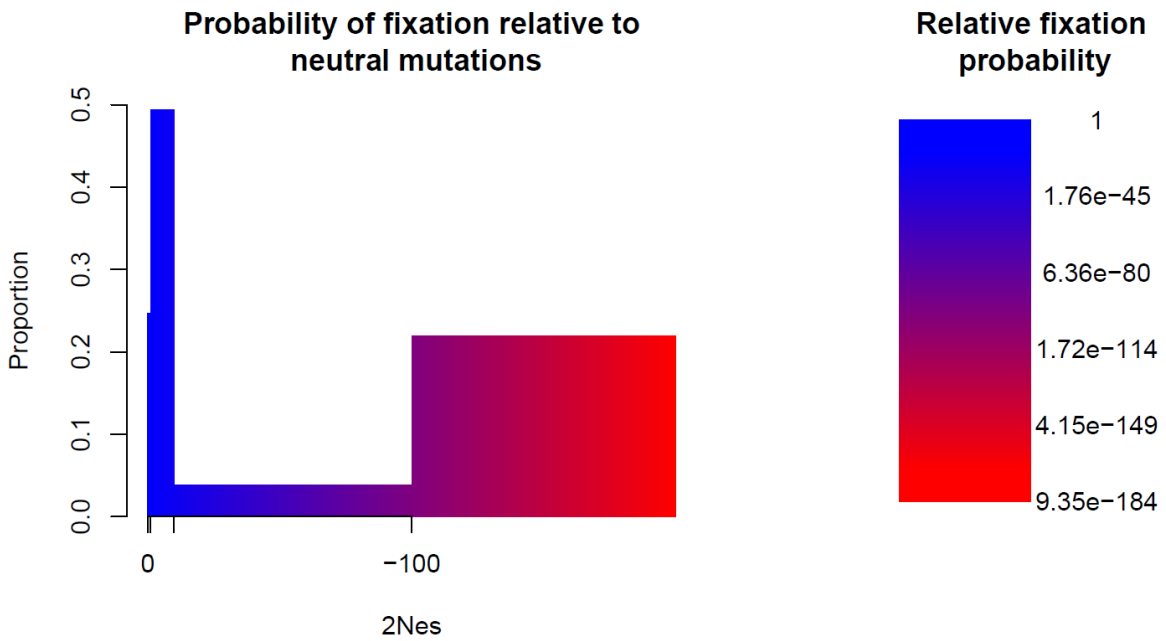

Supp Figure 1: Shown above is the specific DFE of deleterious mutations assumed in this study (from Johri *et al.* 2020), color-coded to display the probability of fixation of deleterious mutations relative to the probability of fixation of neutral mutations. Mutations with selective effects shown in blue regions have an appreciable probability of fixation, while those shown in red are highly unlikely to fix (scale is displayed on right).

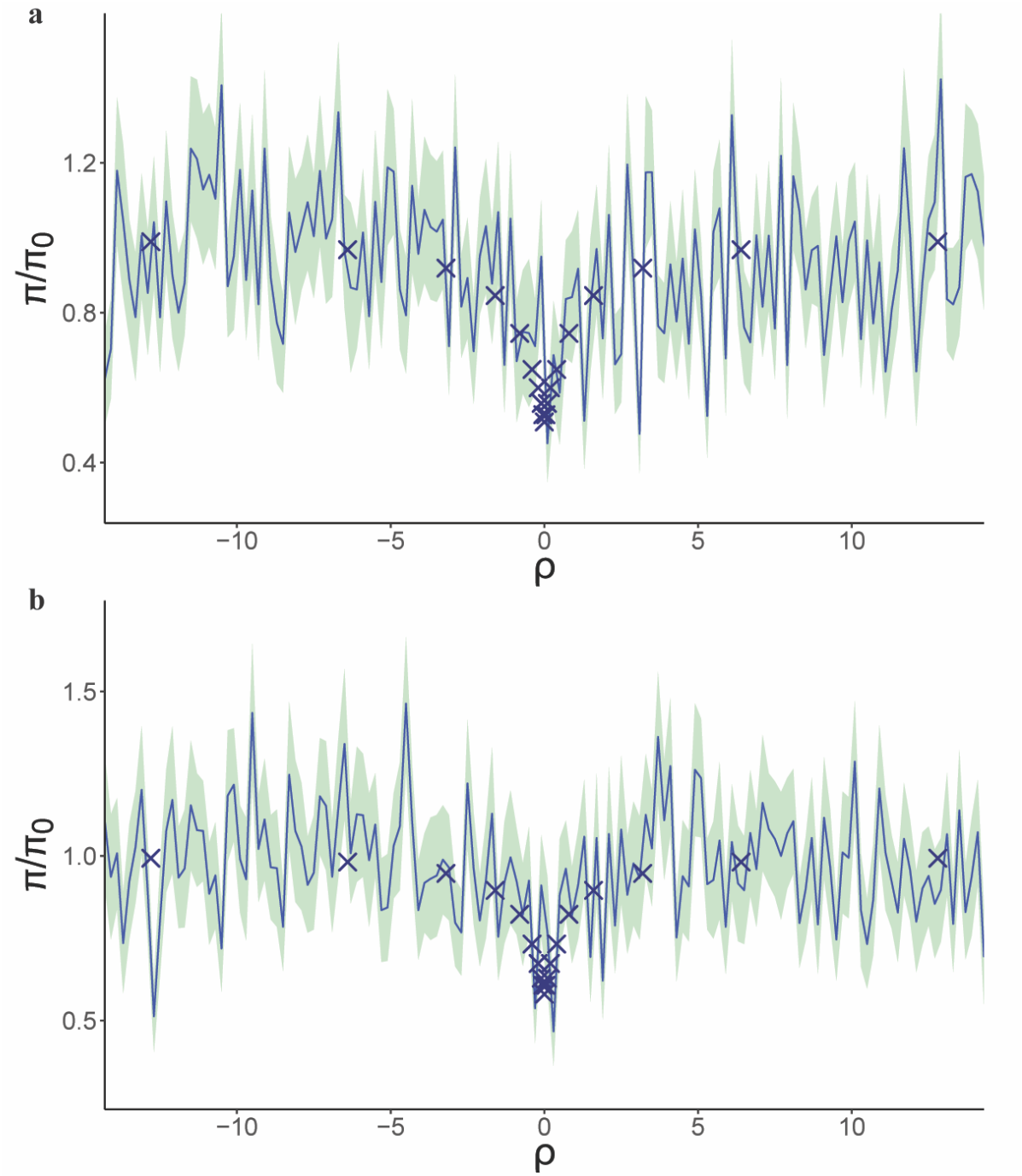

Supp Figure 2: Reduction in neutral diversity from the selected site, post-fixation of a mutation, with $2Ns_a = 5$ and (a) $h = 0$ and (b) $h = 1$. Solid lines represent mean values of 100 replicates, shaded regions correspond to 1 SE above and 1 SE below the mean. Crosses correspond to simulations based on equations (27) of Tajima (1990).

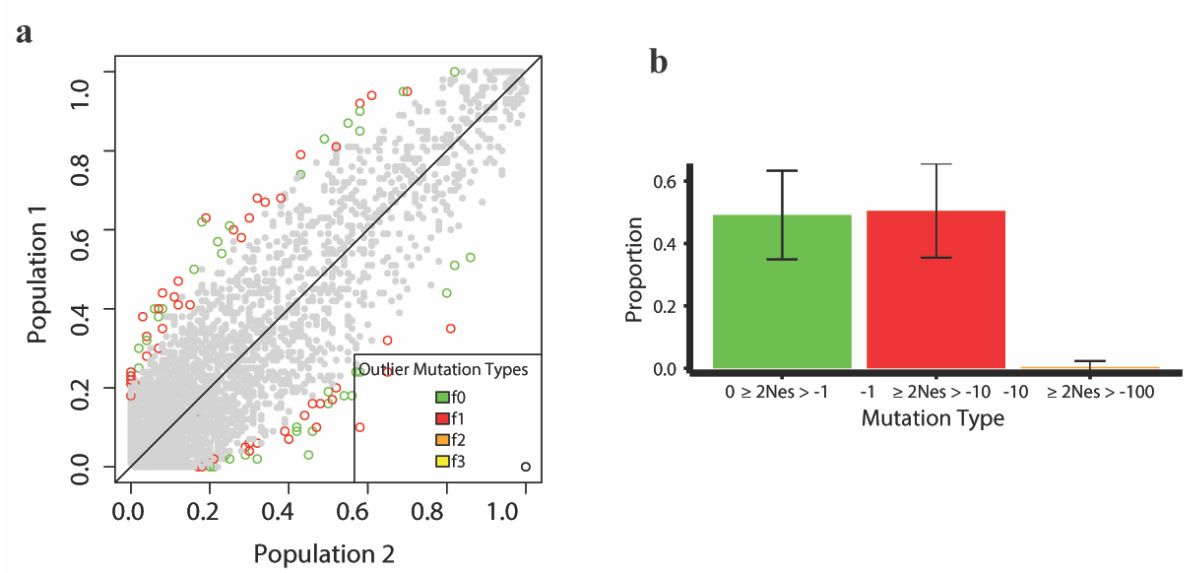

Supp Figure 3: Allele frequencies of SNPs in European (population 1) *vs* African (population 2) populations - under the parameters inferred by Arguello *et al.* (2019), and where the selective effects of all mutations are not re-scaled after the split (thus selection is stronger in the African population). Simulated genomic elements experience purifying selection given by the DFE inferred in Johri *et al.* (2020). Colored open circles represent outliers. Green depicts effectively neutral mutations while warm colors depict deleterious mutations, with red representing weakly deleterious mutations. *Left panel*: Allele frequency plots are shown for 10 (out of 100) replicates. *Right panel*: The distribution of fitness effects of outlier mutations displaying the mean and standard deviation for all 100 replicates.

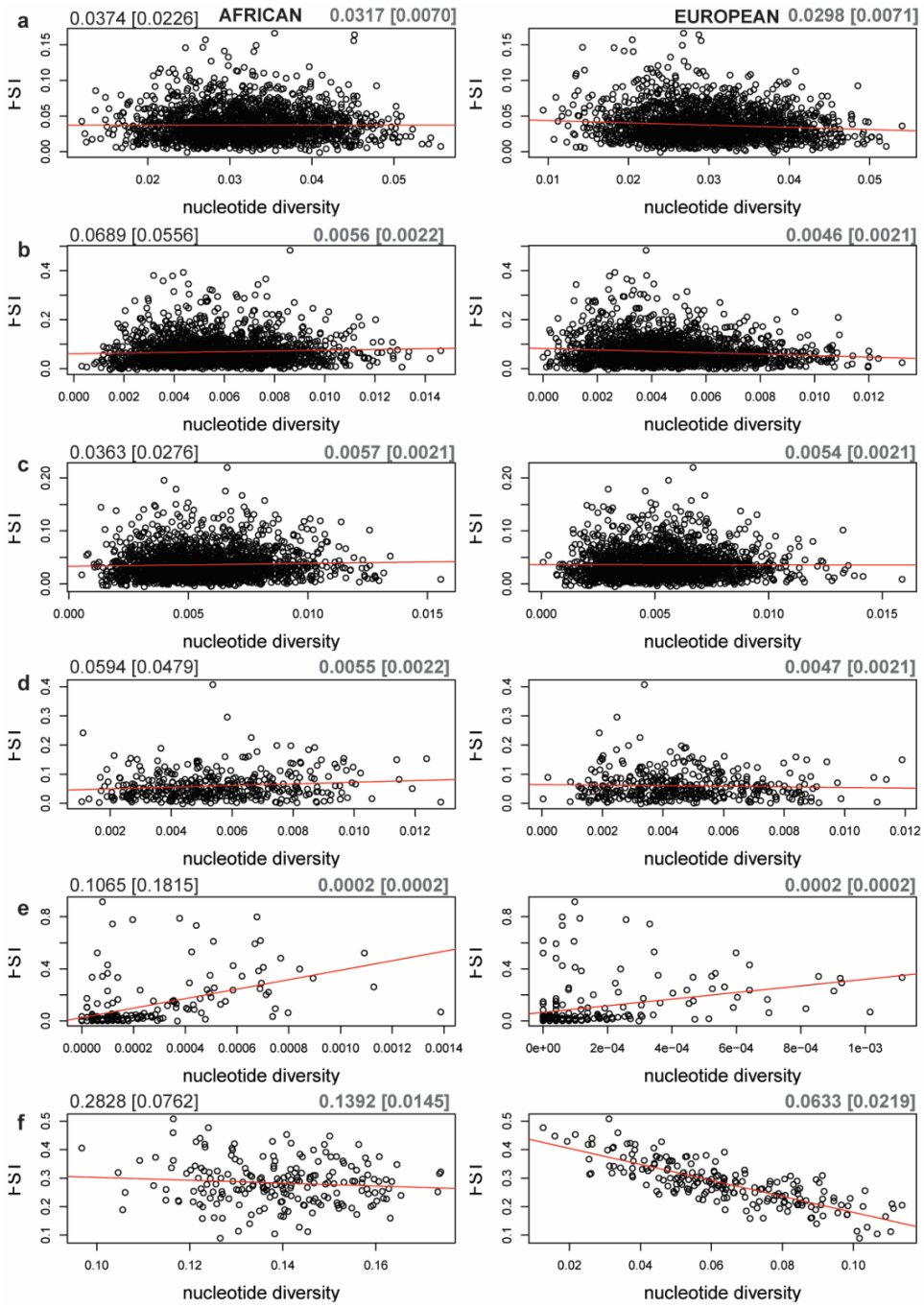

Supp Figure 4: The relationship between F_{ST} and nucleotide diversity calculated for neutral mutations alone, for the African and European populations simulated under six scenarios: (a) neutrality, (b) purifying selection (rescaled DFE), (c) purifying selection (not rescaled DFE), (d) purifying selection and weak positive selection, (e) purifying selection and strong positive selection, and (f) the neutral bottleneck of Li & Stephan 2006. On each, the upper left corner gives mean F_{ST} values with the SD in parentheses. The upper right corners give the corresponding mean value of π with the SD in parentheses. The red line represents the best fitting linear regression. Note the difference in scale between scenarios.

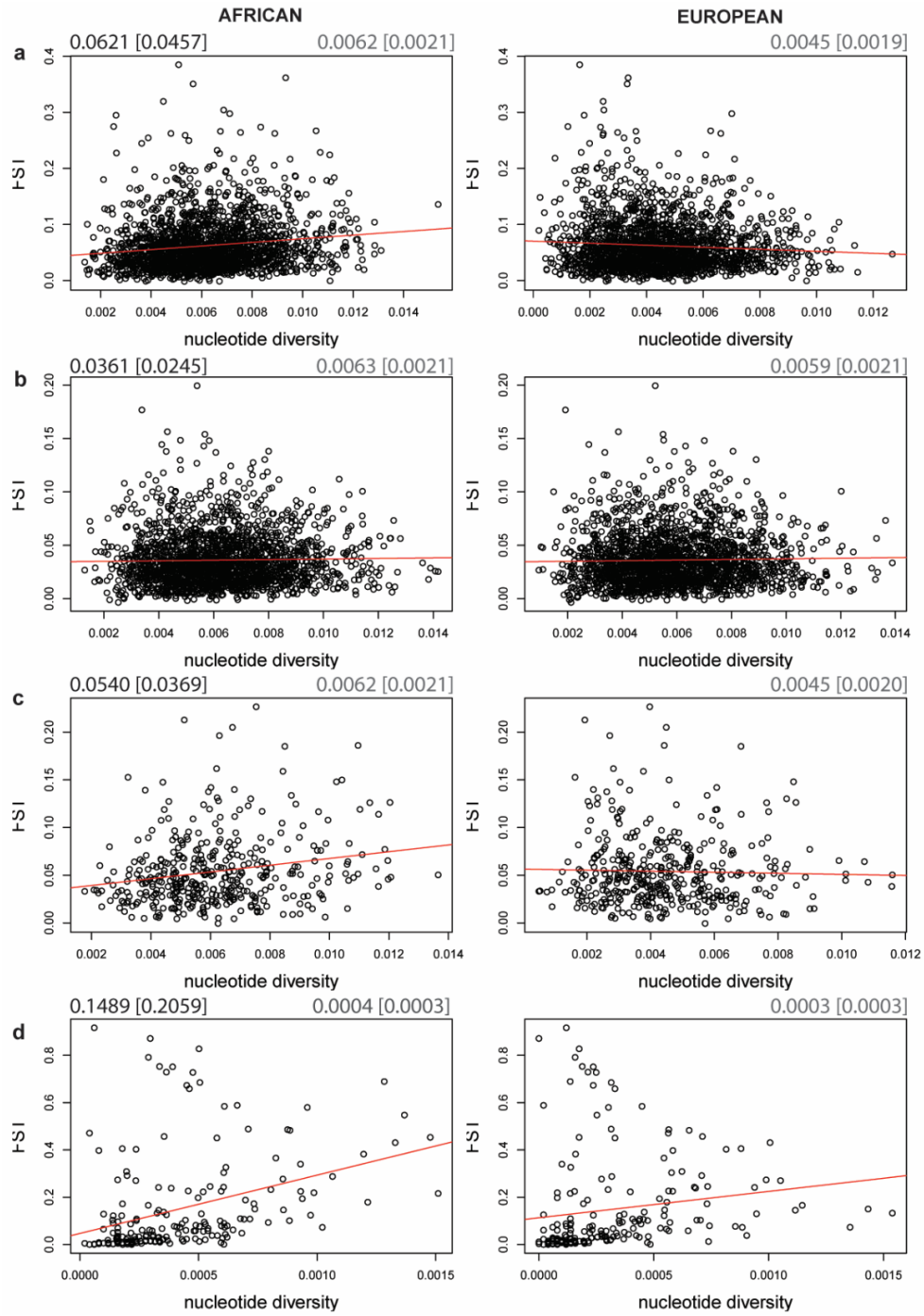

Supp Figure 5: The relationship between F_{ST} and nucleotide diversity calculated for weakly deleterious mutations alone, in the African and European populations simulated under four scenarios: (a) purifying selection (rescaled DFE), (b) purifying selection (not rescaled DFE), (c) purifying selection and weak positive selection, and (d) purifying selection and strong positive selection. On each, the upper left corner gives mean F_{ST} values with the SD in parentheses. The upper right corner gives the corresponding mean value of π with the SD in parentheses. The red line represents the best fit linear regression. Note the difference in scale between scenarios.

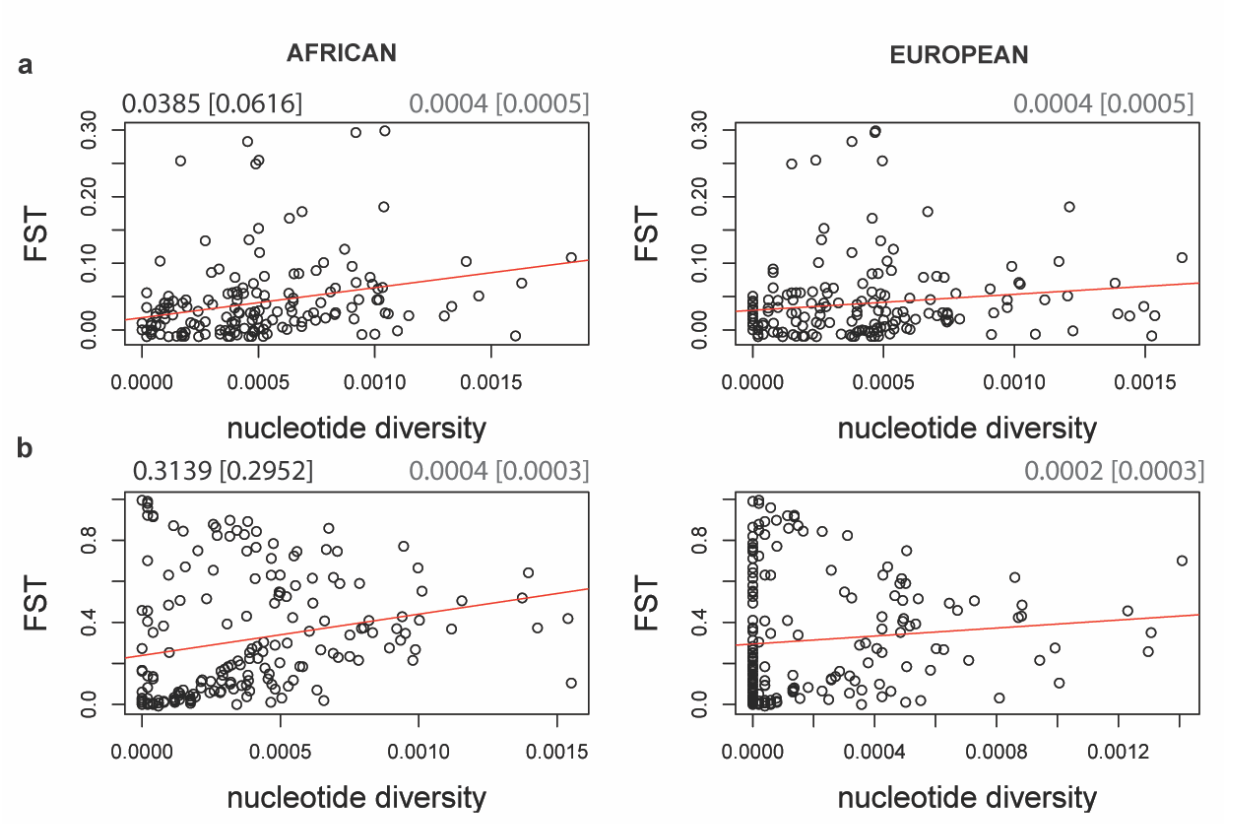

Supp Figure 6: The relationship between F_{ST} and nucleotide diversity calculated for only beneficial mutations in the African and European populations simulated under two scenarios: (a) purifying selection and weak positive selection, and (b) purifying selection and strong positive selection. On each, the upper left corner gives mean F_{ST} values with the SD in parentheses. The upper right corner gives the corresponding mean value of π with the SD in parentheses. The red line represents the best fit linear regression. Note the difference in scale between scenarios.